Analytical and Finite Element Evaluation for the Buckling Characteristics of Laminated Composite Shells

A Dissertation Submitted
in partial Fulfillment of the Requirements
for the Award of the Degree of

MASTER OF ENGINEERING

in

CAD/CAM Engineering

by

Honey Neeraj

801684004

Under Supervision of:

Dr. Neeraj Grover
Assistant Professor
Mechanical Engineering Department

Dr. Kishore Khanna
Assistant Professor
Mechanical Engineering Department

MECHANICAL ENGINEERING DEPARTMENT
THAPAR INSTITUTE OF ENGINEERING AND TECHNOLOGY
(DEEMED TO BE UNIVERSITY), PATIALA-147004, PUNJAB, INDIA
July 2018

Certificate

This is to certify that the work done in this thesis report titled **"Analytical and Finite Element Evaluation for the Buckling Characteristics of Laminated Composite Shells"** submitted in partial fulfillment of requirement for the award of Master of Engineering degree in CAD/CAM Engineering in the Mechanical Engineering Department of Thapar Institute of Engineering and Technology, Patiala, is an authentic record of work carried out by me under the guidance of **Dr. Neeraj Grover** and **Dr. Kishore Khanna**, Mechanical Engineering Department, Thapar Institute of Engineering and Technology, Patiala. The matter embodied in this report has not been submitted in any part or full to any other university or institute for the award of any degree.

Honey Neeraj

Roll. No. 801684004

This is to certify that above declaration made by the student concerned is correct to the best of my knowledge and belief.

Dr. Neeraj Grover
Assistant Professor
MED
Dated: 21/8/2018

Dr. Kishore Khanna
Assistant Professor
MED
Dated: Aug 21, 2018

Dedicated to

My Parents

Acknowledgement

I would like to specially acknowledge and extend my heartfelt gratitude to all those who have helped me in completion of this seminar thesis report. With the biggest contribution, I would like to thank **Dr. Neeraj Grover** sir and **Dr. Kishore Khanna** sir for their time, support and encouragement throughout course of this studies. I have learned so much from them and look forward to their continuous support future endeavours in life.

Lastly, I would also like to thank my parents for their years of unyielding love and encourage. They have always wanted the beat for me and I admire their determination and sacrifice.

Honey Neeraj

Abstract

Laminated composite shell panels are increasingly used in engineering applications such as aeronautical, marine and mechanical industries as well as in other fields of modern technology because of its advance mechanical properties. Shell structures are light in weight and have increased structural stiffness as compared to plates. Composite material has increased the performance and reliability of structural systems and addition to that using shell structure further advances it. The advantage of using shell structure is due their curvature their ability to carry loads and bending action increases. Buckling is one of the important mode of failure in engineering designs thus the need to study the buckling in shells arises. If any structure has a region of compression, then there is a possibility of buckling to occur. This study focuses on the analysis of buckling of composite shell structure using higher order shear deformation theory. There are several theories that have been developed regarding the analysis. In this work the mathematical model based on a new inverse hyperbolic shear deformation theory for buckling analysis of composite shells is used. To ensure the accuracy of the mathematical model to be developed Navier type solution incorporated. The equations developed are to be coded in MATLAB for buckling response of composite shell structure. The laminated composite shells are modelled in the finite element framework and compared with the results of closed form solution only for the simply supported condition. The effects of thickness ratio, aspect ratio, curvature ratio, the angle at which the layers are kept, number of layer and the material properties on the buckling responses are to be studied in detail.

Keywords: Composite material, Buckling, Shell structure, IHSDT, Navier technique, Finite element method.

Table of Contents

List of Figures

List of Tables

Nomenclature

x_1,x_2,x_3	Cartesian coordinates
$\bar{u}$, $\bar{v}$, $\bar{w}$	In-plane displacements
u,v,w	Mid-plane displacements
a,b,h	Length, breadth and thickness of shell
R_1,R_2	Radius of curvature
r	Constant
a_1,a_2	Vector tangents
$[\bar{Q}_{ij}]^{(k)}$	Transformed reduced stiffness matrix
E	Elasticity coefficient
G	Rigidity coefficient
v	Poisons ratio
U	Strain energy
V	Work done
N,M,P	In-plane stress, moment and higher order moment resultant
R	Resultant stiffness matrix
F	Force vector
K_G	Global geometric stiffness matrix
G	Geometric stiffness matrix
q	Transverse load

Greek Symbols

ϕ_1 , ϕ_2	Shear rotations
θ	Angle of fibre orientation
ε_1 , ε_2	Normal strains
ε_6	In-plane shear strain

ε_4 , ε_5	Transverse shear strains
ξ_1, ξ_2, ξ_3	Surface coordinates
$\varepsilon_L, \varepsilon_{NL}$	Linear strain and non-linear strain
λ	Buckling load parameter
σ	Normal stress
Δ	Displacement vector

Acronyms

CLPT	Classical laminate plate theory
FSDT	First order shear deformation theory
HSDT	Higher order shear deformation theory
IHSDT	Inverse hyperbolic shear deformation theory
CFS	Closed form solution
SSSS	Simply supported boundary condition
CCCC	Clamped boundary condition
MP	Material property
NDBL	Non-dimensional buckling load
FEM	Finite element method

CHAPTER 1

INTRODUCTION

1.1 Composite Materials

At present laminated composite panels and shell structure are broadly used in application such as ship frames, racing car frame and storage reservoirs etc. The growing usage of laminated composite shell panels can be observed in marine and field projects. The two principal constituents of composites are matrix and reinforcement as illustrated in Fig 1.1.

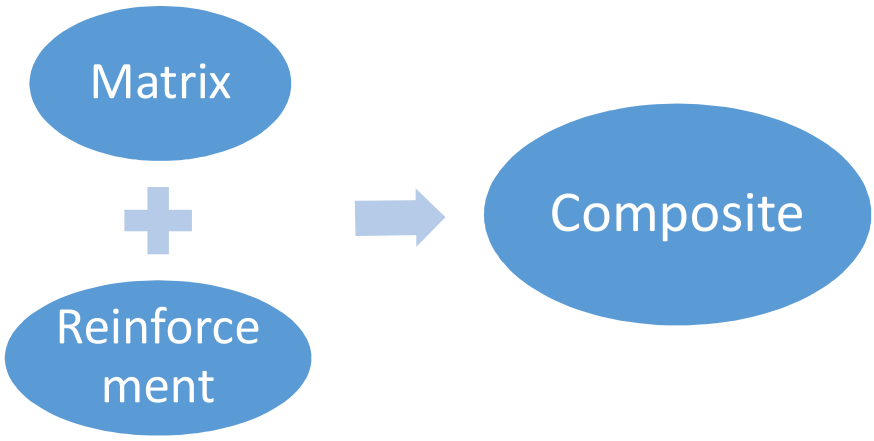

Figure 2.1 Constituents of composite material

Matrix provides insurance and support for the reinforcements and in all direction the load is distributed uniformly. The primary function of the reinforcement is to carry the load. Laminated composites are lightweight when compared to wood, concrete and metal which are traditional materials. That's why laminated composites have broad applications in aerospace, modern automobile, naval and modern structure. Composite materials have properties, for example, its volume to its weight proportion, low coefficient of thermal expansion, amazing versatile properties and resistance to corrosion and synthetic compounds safe which makes them alluring for the researchers. Laminated composites panels are piled up which can be employed for a special purpose. The composites have a capability to provide the tailored properties for the structural design as per requirements for elite designing applications. There is advanced composite material known as FGM (Functionally graded material). Functionally graded materials (FGMs), a kind of composites, are obtained by mixing ceramic and metal in proportion that vary continuously as a function of position along certain dimension(s) of the structure [Khanna *et al.* (2015) and (2017)].

A shell panel is a curved surface. The manufacturing of the shell may be from single layer of material or from the multi-layer isotropic or anisotropic materials. The shell structures are divided into different categories on the basis of the radius of curvatures such as doubly curved shells, cylindrical shells, spherical (in which both of the radius are matched), conical shells (one curvature is equal to zero and the other with the axial length changes linearly), and plate (curvatures are having infinite value). The membrane stiffness of the shell panel is substantially higher than that of the bending stiffness this is because without large deformations it can withstand a considerable amount of membrane strain energy. The outer skins of aircraft/spacecraft/automobile are composed of the thin laminated composites having panel type of geometry. The structural machinery of rapid flying machine, rockets and launch vehicles are dealt with the extreme loading resulting in the aerodynamic heating in course of the function consequently structural responses for example deformations natural frequencies and buckling are influenced substantially. When a shell is exposed to a compressive load, as a result strain energy will be accumulated and eventually leads to bending in the structure on further increment of load, progressively prompts the structure to undergo buckling failure. Henceforth, the buckling demonstrates a crucial role in the building outline and analysis of the structural components. There are mainly two types of buckling firstly eigenvalue buckling while the other is limit point buckling. At the point when the structure is presented to buckling, it doesn't imply that it will fail without a doubt however rather it will have the capacity to convey more load past its ability.

1.2 Classification of Composites

On the basis of the reinforcements used, composites can be categorised as follows:

a) Particulate reinforced composites
b) Fibre reinforced composites

a) Particulate Reinforced Composite consists of particles inundated in alloys and ceramics matrices. They have preferred standpoint of enhanced quality, hoisted working temperature and free from oxidation. Typical examples are gravel, sand and cement to make concrete, silicon carbide particles in aluminium.

b) Fibre Reinforced Composite consists of matrices reinforced by short (discontinuous) or long (continuous) fibres. Fibres give strength to the matrix phase. Examples of fibres are carbon and aramid

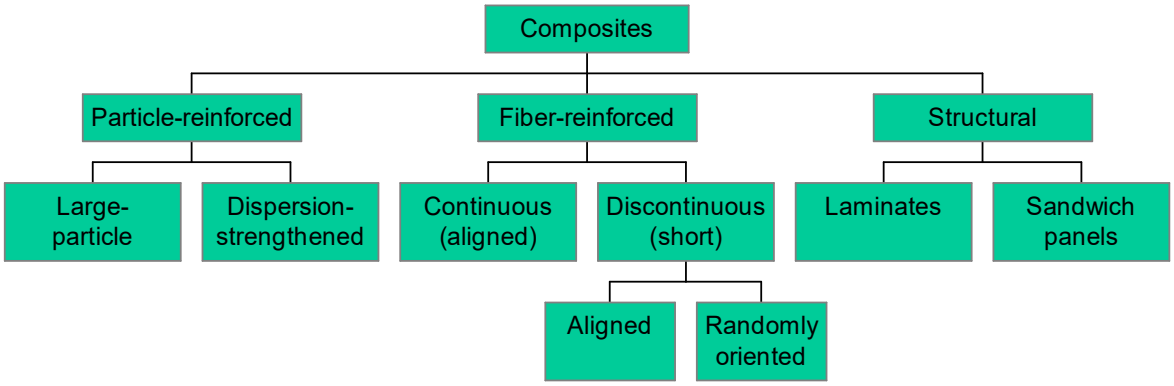

Figure 1.2 Classification of composites

Composites are likewise ordered based on material of matrix as:

a) Metal matrix composite (MMC)
b) Ceramic matrix composite (CMC)
c) Polymer matrix composite (PMC)

a) Metal Matrix Composites

Metal matrix composites have a few favourable advantages when compared to monolithic metals like higher specific modulus, higher specific strength, improved properties at lifted temperatures, and low values of coefficient of thermal expansion. As a result of these qualities metal framework composites are under consideration for extensive number of uses, viz. in rocket, space carry, lodgings, hose, links, heat exchangers and so on.

b**) Ceramic Matrix Composites**

Toughness increment is one of the fundamental idea behind manufacturing ceramic matrix composites. Naturally, it is anticipated and in reality often discovered that there is a conjoined increase in strength and stiffness.

c) Polymer Matrix Composites

Polymers are a standout amongst the most utilized matrix material. The explanations behind this are twofold. In general, polymers have inadequate mechanical properties for any structural purposes. Specifically, their strength and stiffness have a lower value when compared to metals and ceramics.

1.3 Merits of Composites

- When compared to steel and aluminium the composite materials have greater tensile strength (four to six times).
- Torsional stiffness and impact properties are better in composites.
- The Fatigue endurance limit is higher which is 60% of the ultimate strength.
- Composites are lighter material i.e. 30%-40% lighter and cane be substitute with the aluminium structure with the same functional requirement.
- Embedded energy is lower than that of the basic metallic materials like steel, aluminium so on.
- Composites create less noise when in task and produce low estimation of vibrations transmission when compared with metals.
- Composites are flexible materials than metals and can be tailored as indicated by the need and prerequisite.
- Due to their long life, good fatigue, impact, resistance to environment and reduce maintenance can be obtained.
- Life-cycle cost is less in composites when compared to metals.
- Composites are resistant to corrosion and damage due to fire.
- Aesthetics are better than metal and can be readily used as decorative.

1.4 Applications of Composites

- Aerospace industry
- Sporting Goods Industry
- Automotive Industry
- Home Appliance Industry
- Communication antenna, electronic circuit and boards
- Safety equipment like ballistic protection and airbags in cars.

There is a wide application of composites in the aerospace industry. The outer layer of aircraft/spacecraft/automobile are made of the thinly laminated composites having panel type of geometry. The structural machinery of high-speed aircraft, shuttles and launch vehicles are

exposed to extraordinary loading because the aerodynamic heating in course of their administration, therefore, the basic reactions, for example, deformation, buckling and natural frequencies are influenced fundamentally.

Summary

Due to several merits of composites, it is feasible to use composites in the aerospace industry widely. Thus the study of composite material arising these days.

CHAPTER 2

LITERATURE REVIEW

2.1 Introduction

The buckling characteristics of composite shells have been studied by many researchers either using analytical methods or numerical methods. The term buckling can be defined as the load on a structure when a compressive stress is applied on it. Buckling is an important mode of failure thus numerous investigation have been carried out in the literature. There are many theories that have been developed to study the shear deformation of composites. The three broad categories are:

a) The classical laminate plate theory (CLPT)
b) The first-order shear deformation theory (FSDT)
c) The higher-order shear deformation theory (HSDT)

There are lots of literature on buckling of composite shell structure from which some of them are discussed below.

2.2 Shear Deformation Theories

Pagano (1970) and Srinivas (1970) provided the exact 3-D solutions for the structural analysis of materials. Though it has provided the exact solution but the computational cost was very high so the equivalent single layer theory was developed in which the 3-D problem was approximated as 2-D problem for simplification.

The classical laminate plate theory was first presented by Love (1927). This theory presented good outcomes for thin plates however CLPT overlooks the transverse shear impact therefore it isn't appropriate for the decently thick plates or shells. Thus, CLPT was not suitable for the thick plates or shells analysis in which the transverse shear effect is considerable.

Koiter (1960) proposed the theory for elasticity on thin shells which was based on the energy considerations. In this theory, transverse shear stresses were also incorporated.

Applications of theory proposed by Love to multi-layered structures was done by Reissner and Stavwsky (1961). The effect of transverse shear stresses was neglected in this model.

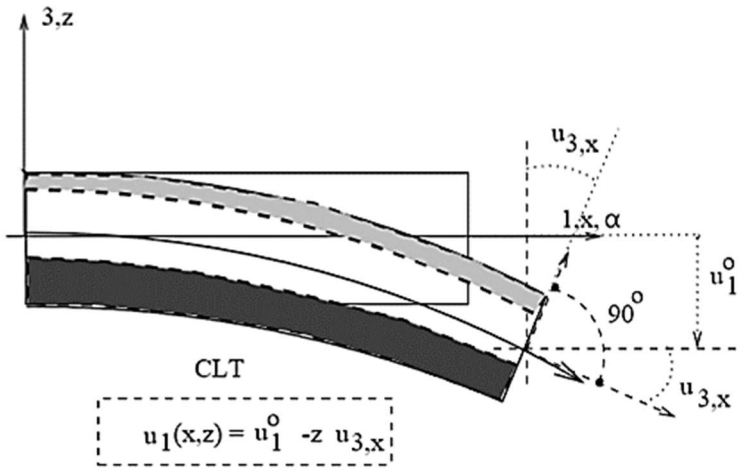

Figure 2.1 Displacement Model of CLPT [Carrera, 2002]

Reissner (1945) and Mindlin (1951) proposed a model, which also consider transverse shear strains are known as the First order shear deformation theory. The assumptions utilized as a part of CLPT were refined in the FSDT model. The displacement field in terms of mid-plane displacements (u_0, v_0, w_0) of FSDT are:

$$u = u_0 + z\phi$$
$$v = v_0 + z\phi$$
$$w = w_0$$

The displacements at any point in the Cartesian coordinates is denoted by the parameters u, v and w. The term ϕ represents the rotation between the two normal as depicted in Figure 2.2.

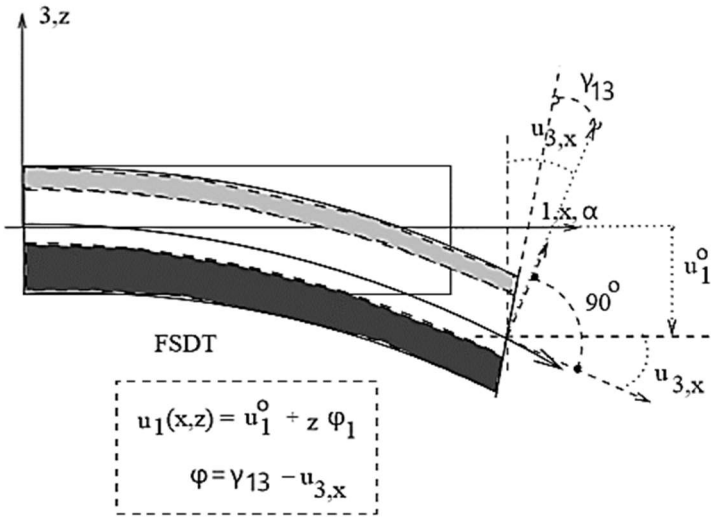

Figure 2.2 Displacement model of FSDT [Carrera,2002]

The transverse shear effect was not found to be zero at the top and the bottom of the plate in FSDT.

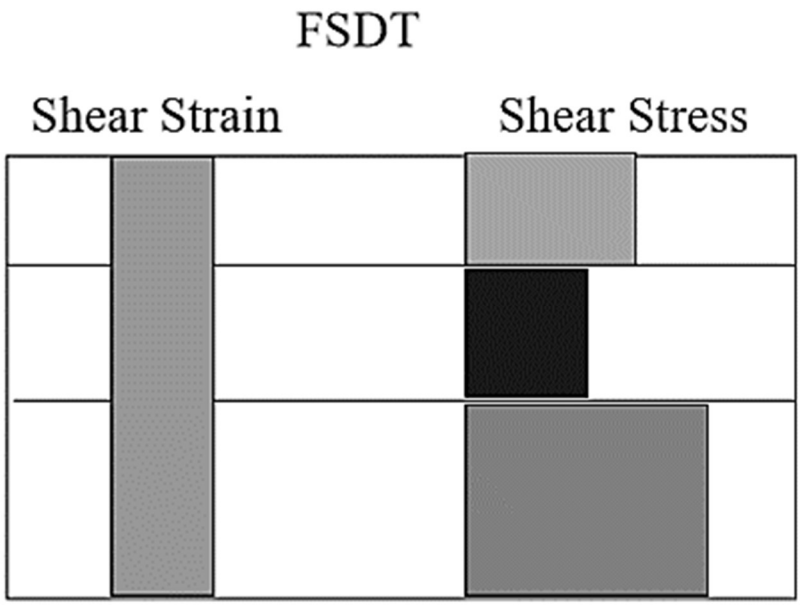

Figure 2.3 Distribution of shear stain and stresses in FSDT [Carrera, 2002]

In Figure 2.3 it should be observed that the effect of transverse shear is constant along the thickness and discontinuous at the layer interface. Thus, the requirement for the shear correction factor in FSDT was required. It increased the computation as it depends upon various parameter.

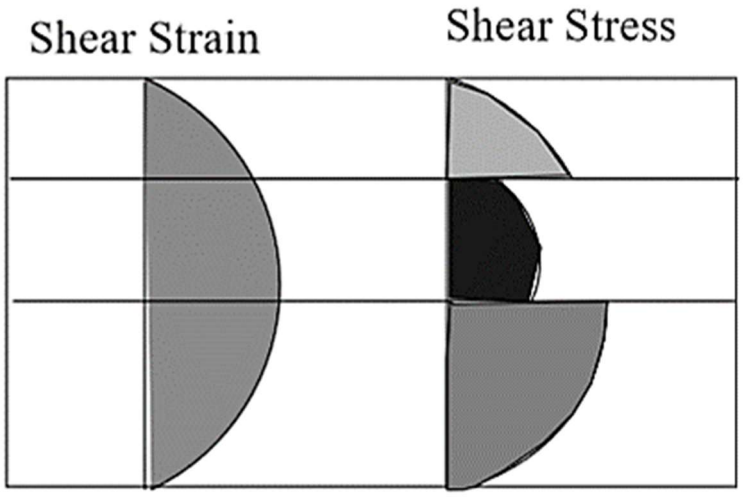

Figure 2.4 Distribution of Shear strain and stresses in HSDT [Carrera,2002]

In Figure 2.4 it can be observed that the shear strain and stresses are equal to zero at the top and the bottom surfaces. It led to extension of FSDT to higher order shear deformation theories. HSDT is divided into two categories:

a) Polynomial Shear Deformation Theory
b) Non-Polynomial Shear Deformation Theory

The Taylor series expansion is utilized in terms of thickness coordinates for the displacement field in Polynomial shear deformation theory. The coefficients of shear rotation in the displacement field represents the higher order terms of thickness coordinate. In Non-polynomial shear deformation theory, a non-polynomial function of the thickness is considered in the displacement field.

2.3 Buckling Analysis of Composite Shells

The importance to study the buckling behaviour of composite shell structure is mandatory since buckling is one of failure mode in plates and shell structure.

Srinivas and Rao (1970) provided an exact solution for the three-dimensional unified analysis for the bending, buckling response and vibration. Rectangular plates which are simply supported is considered and laminates is formulated.

Reddy and Liu (1985) studied the laminated elastic shells using high order shear deformation theory. A high-order shear deformation theory is used to study the laminated shells. The theory represents the parabolic variation of shear strains through thickness. The Navier-type exact solutions for bending and natural vibrations are exhibited for cylindrical and spherical shells. Simple supported boundary conditions are taken. The exact solution of cross-ply shells for deflections and natural frequencies are presented.

Khdeir *et al.* (1989) The cross-ply circular cylindrical shells are analysed for static response, vibration and buckling of the classical theory, first-order theory and third-order shell theory and are obtained using state space approach. The parameters such as boundary conditions effect, layer number and shear deformation on deflections, frequencies, stresses, and buckling loads is shown by comprehending a few numerical illustrations.

Sundaresan *et al.* (1989) the effect of partial edge compression on the buckling behaviour of decently thick laminated composite plates is explored. An eight noded isoparametric plate element is developed for studying two boundary conditions. It is observed that the plates which

are having partially loaded edges act differently in comparison to those subjected to full-edge compression.

Buckling behaviour of composite shells studied using finite element model by Ferreira and Barbosa (2000). The analysis of composite shell structures for geometric non-linear, a finite-element model is used. Marguerre shell element with layered formulation is adopted. The buckling behaviour of composite shells were studied on the basis of various material orientation and stacking laminates. Layer [0] produces much higher buckling load in absence of it flexible behaviour can be seen. However, in laminates [0/90/90/0] or [0/45/-45/0] its influence is negligible.

Prusty and Satsangi (2001) analysed the buckling of composite stiffened plates and cylindrical shells. The buckling behaviour of laminated shell panels exposed to different loading cases are investigated and the results are contrasted with the existing literature.

Kumar *et al*. (2003) analysed the multi laminated curved panels for the study of tensile buckling, vibration and dynamic stability. The panels are subjected to tensile edge loading and uniaxial in-plane point. The results are evaluated through finite element method.

Thinh *et al*. (2005) analysed the Buckling of multi laminated cylindrical shell panels subjected hygrothermal loadings and axial loading. The geometrical non-linear analysis is incorporated utilizing the Finite Element evaluation using single layer first shear deformation theory. The effects of number of layers, lamination angle, ratio of length to width and hygrothermal effects are examined.

Using a new higher order shear deformation theory static and dynamic analysis of laminated composite panels and sandwich plates has been done by Mantari *et al.* (2011). Elastic composite/sandwich plates and curved panels are analysed by adopting developed new HSDT. The new displacement field whose value effected by the parameter “m” whose value is obtained to provide the results closest to the 3D elasticity bending solutions. The boundary conditions and governing equations are derived by adopting the principle of virtual work. A Navier type closed form Solution methodology is used. The shells and plates are subjected different loads such as point, bi-sinusoidal and distributed loads. The results obtained are compared with various available literature which reveals that the performance of present theory is better.

Nguyen-van *et al.* (2011) used a smoothed quadrilateral flat shell element having in plane rotation analysed buckling response and vibration for composite plates and shells within the framework of FSDT. Even the flat element formulation has shown adequate and stable results. The present element used was effective, accurate and free of locking.

Radial basis function for buckling response and vibration analysis of isotropic and laminated plates was used by Ferreira *et al*. (2011). First order shear deformation theory is incorporated to obtain the buckling and vibration response of laminated plates. The radial basis function is used to discretise the boundary conditions and equation of motions which is simple yet powerful alternative for existing methods.

Isotropic and multilayered plates and shells are analysed using generalised high order shear deformation theory is done by Mantari and Soares (2012). Generalised 5 DOF HSDT are introduced to investigate the bending and free vibration of shells and plates. The governing equations and boundary conditions are derived by utilising principle of virtual work. These equations are obtained via Navier-type closed form solutions. Panels are subjected to sinusoidal, distributed and point loads. The results are also compared with the new and other HSDTs and are compared with the exact 3-Dimensional elasticity theory. Shown better results than the other HSDTs.

Mantari *et al.* (2012) introduced a new trigonometric shear deformation theory for the study of laminated composite and sandwich plates. the results are obtained closest to 3D elasticity bending solution by using a displacement field depending upon the parameter 'm'. The theory is utilised for shear strains distributions through the thickness of plate and boundary conditions that are free from tangential stress. The results when compared with the published literature, it shows closest agreement.

Shadmeri *et al.* (2012) analysed buckling of conical composite shell using semi-analytical approach under the compression load. First order shear deformation theory was implemented. Formulation for both axisymmetric and non-axisymmetric have been derived and solved for buckling response.

Grover *et al.* (2013) has done the deflection and buckling analysis of laminated composite plates and sandwich plates using new IHSDT. A new inverse hyperbolic shear deformation theory is introduced and validated for several numerical illustrations. The theory is for laminated composites and sandwich plates for both buckling and static responses. Principle of

virtual work is employed to derive the governing differential equations. A Navier type closed form solution methodology is incorporated for obtaining the solution. The present theory is free from any errors and provide accurate solution.

Fazzolari *et al.* (2013) has used exact solution method using Higher order shear deformation theory to study the buckling of composite plate assemblies. The principle of minimum potential energy for determining the governing equations and boundary conditions is applied and symbolic algebra is used to conduct the buckling analysis in an exact sense. The exact HSDT has shown accurate results and better than FSDT. Introduction of stiffeners effectively in the composite plates considerably effects the buckling load.

Grover *et al.* (2014) The generalized finite element methodology employing inverse trigonometric shear deformation theory is formulated. The structural responses such as static, buckling, and free vibration of laminated-composite and sandwich plates are investigated. The effect of various parameters such as material anisotropy, lamination sequence, loading, aspect ratio and span thickness on structural response is studied.

Joshan *et al.* (2017) The thermos-mechanical response of cross-ply and angle-ply laminated plates is investigated. The work is done under the framework of inverse hyperbolic shear deformation theory. The sinusoidal and transverse loading is considered with linear and non-linear distribution over the thickness of plate. The effect of various parameters such as material anisotropy, lamination sequence, loading, aspect ratio and span thickness on thermo mechanical response is studied.

Joshan *et al.* (2017) A new non-polynomial shear deformation theory having four variables is formulated for the hygro-thermal-mechanical analysis of laminated composite plates. An inverse hyperbolic function of thickness coordinate is used in the displacement field in order to consider the shear deformation effects. The bending response of laminated plates in hygro-thermal environment at lesser computational cost is analysed.

2.4 Gaps in the literature

1. A new inverse hyperbolic shear deformation theory hasn’t used yet for the analysis of shell under buckling load.
2. FEM based analysis of shell structure on the developed mathematical model can't be seen as per the literature review.

2.5 Objectives

This work motive is to formulate a general mathematical model for multi layered composite curved panel i.e. shell structure under buckling load utilizing the IHSDT displacement field model. On the basis of the gaps identified following objectives has been framed:

1. Modelling of composite shells using IHSDT.
2. Buckling analysis of composite shells using IHSDT and analytical solution.
3. Buckling of doubly curved spherical and cylindrical shells.
4. The modelling of composite shell panels and buckling response in the framework of finite element method.

Summary

Based on the literature review, the gaps in the literature were recognised and the objective for the present thesis was framed.

CHAPTER 3
METHODOLOGY

3.1 Introduction

This section is assigned for the modelling of doubly curved composite shells by using inverse hyperbolic shear deformation theory (IHSDT). The governing differential equations are developed using variational approach i.e. principle of virtual work(PVW). A Navier type closed form solution methodology is used to fulfil the boundary conditions. In the present work, the simply supported and cross ply doubly curved composite shells are considered which are exposed to axial compressive forces.

In this study, a panel is supposed to be fabricated of different number of orthotropic layers having uniform thickness *h*. The length is given as *a* and width as *b* as represented in the Figure 3.1 below. Also the principal radii of curvature are denoted by R_1 and R_2.

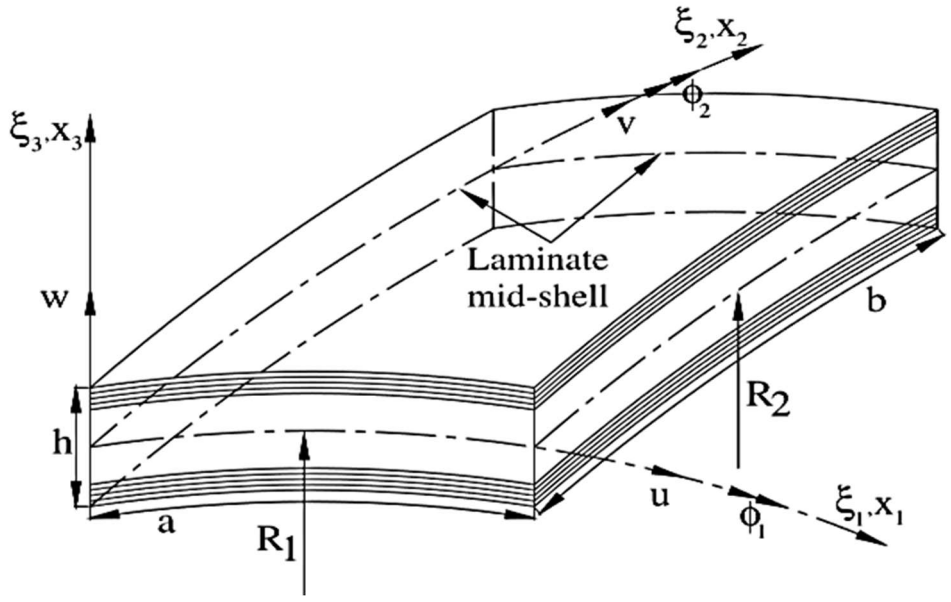

Figure 3.1 Laminated shell geometry [Mantari and Soares, 2012]

3.2 Displacement Field

The shear deformation theory based on inverse hyperbolic function is implemented for modelling and analysis of plates by Grover *et al.* (2013). The given below displacement field for the laminated shell and plates ($R_{1,2}\rightarrow\infty$) established on the IHSDT is designed to obtain the mathematical model. In the present thesis work, the IHSDT is extended to model the shell structure.

$$\begin{aligned}
\bar{u}(\xi_1,\xi_2,\xi_3) &= (1+\frac{\xi_3}{R_1})u+\xi_3\left[\Omega\phi_1-\frac{\partial w}{a_1\partial\xi_1}\right]+f(\xi_3)\phi_1\\
\bar{v}(\xi_1,\xi_2,\xi_3) &= (1+\frac{\xi_3}{R_2})v+\xi_3\left[\Omega\phi_2-\frac{\partial w}{a_2\partial\xi_2}\right]+f(\xi_3)\phi_2\\
\bar{w}(\xi_1,\xi_2,\xi_3) &= w
\end{aligned} \tag{3.1}$$

where *u, v* and *w* denote the displacement functions which are at the middle region of the panel. The parameters ϕ_1 and ϕ_2 represent the shear deformation at the middle plane. The function $f(\xi_3)$ is taken as follows:

$$\begin{aligned}
f(\xi_3) &= g(\xi_3)+\Omega\xi_3\\
g(\xi_3) &= \sinh^{-1}\left(\frac{r\xi_3}{h}\right)\\
\Omega &= -\frac{2r}{h\sqrt{r^2+4}}
\end{aligned} \tag{3.2}$$

where $g(\xi_3)$ is the inverse hyperbolic function of ξ_3 and the parameter Ω is the constant which is evaluated in such a manner that the transverse shear effect is zero at the top and bottom surface of the panel. Thus, there is no requirement to consider the shear correction factor. The

value of parameter *r* is chosen as 3 after optimising and comparing it with the corresponding 3D results [Grover *et al.,* (2013)].

3.3 Strain Displacement Relations

The strain-displacement relation that are utilized in this formulation are written as follows [Mantari *et al.,* (2012)]:

$$\varepsilon_1 = \frac{1}{A_1}\left(\frac{\partial \bar{u}}{\partial \xi_1} + \frac{1}{a_2}\frac{\partial a_1}{\partial \xi_2}\bar{v} + \frac{a_1}{R_1}\bar{w}\right)$$
$$\varepsilon_2 = \frac{1}{A_2}\left(\frac{\partial \bar{v}}{\partial \xi_2} + \frac{1}{a_1}\frac{\partial a_2}{\partial \xi_1}\bar{u} + \frac{a_2}{R_2}\bar{w}\right)$$
$$\varepsilon_4 = \frac{1}{A_2}\frac{\partial \bar{w}}{\partial \xi_2} + A_2\frac{\partial}{\partial \xi_3}\left(\frac{\bar{v}}{A_2}\right)$$
$$\varepsilon_5 = \frac{1}{A_1}\frac{\partial \bar{w}}{\partial \xi_1} + A_1\frac{\partial}{\partial \xi_3}\left(\frac{\bar{u}}{A_1}\right) \tag{3.3}$$
$$\varepsilon_6 = \frac{A_2}{A_1}\frac{\partial}{\partial \xi_1}\left(\frac{\bar{v}}{A_2}\right) + \frac{A_1}{A_2}\frac{\partial}{\partial \xi_2}\left(\frac{\bar{u}}{A_1}\right)$$

where

$$A_1 = \left(1 + \frac{\xi_3}{R_1}\right)a_1$$
$$A_2 = \left(1 + \frac{\xi_3}{R_2}\right)a_2 \tag{3.4}$$

The parameter ε_1 and ε_2 represent the normal strains in x_1 and x_2 directions individually, ε_6 is the shear strain acting in-plane while ε_4 and ε_5 represents the transverse shear strains. $\bar{u}$, $\bar{v}$ and $\bar{w}$ are the displacements on the surface and a_1 and a_2 represent the vectors tangent to the ξ_1 and ξ_2 coordinate lines. The Equation (3.1) are introduced in the Equation (3.3) which yields the following strain-displacement relation:

$$\varepsilon_1 = \varepsilon_1^0 + \xi_3\varepsilon_1^1 + f(\xi_3)\varepsilon_1^2$$
$$\varepsilon_2 = \varepsilon_2^0 + \xi_3\varepsilon_2^1 + f(\xi_3)\varepsilon_2^2$$
$$\varepsilon_6 = \varepsilon_6^0 + \xi_3\varepsilon_6^1 + f(\xi_3)\varepsilon_6^2$$
$$\varepsilon_4 = \Omega\varepsilon_4^0 + f'(\xi_3)\varepsilon_4^3 \tag{3.5}$$
$$\varepsilon_5 = \Omega\varepsilon_5^0 + f'(\xi_3)\varepsilon_5^3$$

where

$$\varepsilon_1^0 = \frac{\partial u}{\partial x_1} + \frac{w}{R_1}, \varepsilon_1^1 = \Omega \frac{\partial \phi_1}{\partial x_1} - \frac{\partial^2 w}{\partial x_2^2}, \varepsilon_1^2 = \frac{\partial \phi_1}{\partial x_1}$$
$$\varepsilon_2^0 = \frac{\partial v}{\partial x_2} + \frac{w}{R_2}, \varepsilon_2^1 = \Omega \frac{\partial \phi_2}{\partial x_2} - \frac{\partial^2 w}{\partial x_2^2}, \varepsilon_2^2 = \frac{\partial \phi_2}{\partial x_2}$$
$$\varepsilon_6^0 = \frac{\partial v}{\partial x_1} + \frac{\partial u}{\partial x_2}, \varepsilon_6^1 = \Omega \frac{\partial \phi_2}{\partial x_1} + \Omega \frac{\partial \phi_1}{\partial x_2} - 2\frac{\partial^2 w}{\partial x_1 \partial x_2}, \varepsilon_6^2 = \frac{\partial \phi_2}{\partial x_1} + \frac{\partial \phi_1}{\partial x_2} \quad (3.6)$$
$$\varepsilon_4^0 = \phi_2, \varepsilon_4^3 = \phi_2$$
$$\varepsilon_5^0 = \phi_1, \varepsilon_5^3 = \phi_1$$

3.4 Stress Strain Relations

For every K^{th} Lamina, the stress-strain relations are provided by Reddy (2004),

$$\begin{Bmatrix} \sigma_1 \\ \sigma_2 \\ \sigma_6 \\ \sigma_4 \\ \sigma_5 \end{Bmatrix}_{(k)} = \begin{bmatrix} \overline{Q_{11}} & \overline{Q_{12}} & \overline{Q_{16}} & 0 & 0 \\ \overline{Q_{12}} & \overline{Q_{22}} & \overline{Q_{26}} & 0 & 0 \\ \overline{Q_{16}} & \overline{Q_{26}} & \overline{Q_{66}} & 0 & 0 \\ 0 & 0 & 0 & \overline{Q_{44}} & \overline{Q_{45}} \\ 0 & 0 & 0 & \overline{Q_{45}} & \overline{Q_{55}} \end{bmatrix}_{(k)} \begin{Bmatrix} \varepsilon_1 \\ \varepsilon_2 \\ \varepsilon_6 \\ \varepsilon_4 \\ \varepsilon_5 \end{Bmatrix}_{(k)} \quad (3.7)$$

Where

$$Q_{11} = \frac{E_1}{1 - \nu_{12}\nu_{21}}$$
$$Q_{12} = \frac{\nu_{12} E_2}{1 - \nu_{12}\nu_{21}} \quad (3.8)$$
$$Q_{22} = \frac{E_2}{1 - \nu_{12}\nu_{21}}$$
$$Q_{66} = G_{12}; Q_{44} = G_{23}; Q_{55} = G_{13}$$

$$
\begin{aligned}
\overline{Q}_{11} &= Q_{11}\cos^4\theta + 2\left(Q_{12}+2Q_{66}\right)\sin^2\theta\cos^2\theta + Q_{22}\sin^4\theta \\
\overline{Q}_{12} &= \left(Q_{11}+Q_{22}-4Q_{66}\right)\sin^2\theta\cos^2\theta + Q_{12}\left(\sin^4\theta+\cos^4\theta\right) \\
\overline{Q}_{22} &= Q_{11}\sin^4\theta + 2\left(Q_{12}+2Q_{66}\right)\sin^2\theta\cos^2\theta + Q_{22}\cos^4\theta \\
\overline{Q}_{16} &= \left(Q_{11}+Q_{12}-2Q_{66}\right)\sin\theta\cos^3\theta + \left(Q_{12}-Q_{22}+2Q_{66}\right)\sin^3\theta\cos\theta \\
\overline{Q}_{66} &= \left(Q_{11}+Q_{22}-2Q_{12}-2Q_{66}\right)\sin^2\theta\cos^2\theta + Q_{66}\left(\sin^4\theta+\cos^4\theta\right) \\
\overline{Q}_{44} &= Q_{44}\cos^2\theta + Q_{55}\sin^2\theta \\
\overline{Q}_{45} &= \left(Q_{55}-Q_{44}\right)\sin\theta\cos\theta \\
\overline{Q}_{55} &= Q_{55}\cos^2\theta + Q_{44}\sin^2\theta \\
\overline{Q}_{26} &= \left(Q_{11}+Q_{12}-2Q_{66}\right)\sin^3\theta\cos\theta + \left(Q_{12}-Q_{22}+2Q_{66}\right)\sin^3\theta\cos\theta
\end{aligned}
\tag{3.9}
$$

The stress components are represented as σ_1, σ_2, σ_6, σ_4 and σ_5 and the strain components are given as ε_1, ε_2, ε_6, ε_4, and ε_5. The matrix Q_{ij} is depended upon the fibre orientation and material properties.

3.5 Derivation of shell equations

The governing differential equations for the static and buckling evaluation of composite shells are purposed using the principle of virtual work as follows:

$$
\int_0^T \left(\delta U - \delta V\right) dt = 0 \tag{3.10}
$$

where δU represents the virtual strain energy and δV represents the virtual work done such as:

$$
0 = \int_{\frac{-h}{2}}^{\frac{h}{2}} \left\{ \int_{\Omega}^{(k)} \left[\sigma_1 \delta\varepsilon_1^{(k)} + \sigma_2 \delta\varepsilon_2^{(k)} + \sigma_6 \delta\varepsilon_6^{(k)} + \sigma_4 \delta\varepsilon_4^{(k)} + \sigma_5 \delta\varepsilon_5^{(k)} \right] dx_1 dx_2 \right\} d\xi_3 - \int_{\Omega} q\,\delta w dx_1 dx_2 \tag{3.11}
$$

By solving the above equation with the help of fundamentals of the calculus of variation, the governing differential equations for buckling results are identified in terms of resultant stresses, moments and higher order moments. Setting the coefficients of δu, δv, δw, $\delta\phi_1$, $\delta\phi_2$ to zero respectively, these equations are obtained and are stated in Eq. (3.12).

$$\frac{\partial N_1}{\partial x_1}+\frac{\partial N_6}{\partial x_2}=0$$

$$\frac{\partial N_2}{\partial x_2}+\frac{\partial N_6}{\partial x_1}=0$$

$$-\frac{N_1}{R_1}-\frac{N_2}{R_2}+\frac{\partial^2 M_1}{\partial x_1^2}+\frac{\partial^2 M_2}{\partial x_2^2}+2\frac{\partial^2 M_6}{\partial x_1 \partial x_2}=q+\overline{N}_{xx}\frac{\partial^2 w_0}{\partial {x_1}^2}+2\overline{N}_{xy}\frac{\partial^2 w_0}{\partial x_1 \partial x_2}+\overline{N}_{yy}\frac{\partial w_0}{\partial x_1}$$

$$\frac{\partial P_1}{\partial x_1}+\frac{\partial P_6}{\partial x_2}+\Omega\frac{\partial M_1}{\partial x_1}+\Omega\frac{\partial M_6}{\partial x_2}-Q_1-K_1=0$$

$$\frac{\partial P_2}{\partial x_2}+\frac{\partial P_6}{\partial x_1}+\Omega\frac{\partial M_2}{\partial x_2}+\Omega\frac{\partial M_6}{\partial x_1}-Q_2-K_2=0 \qquad (3.12)$$

where, the resultants of the following integrations give the value of N_i, M_i, P_i, Qi and K_i:

$$\left(N_i, M_i, P_i\right)=\sum_{k=1}^{N}\int_{\frac{-h}{2}}^{\frac{h}{2}}\sigma_i\left(1, \xi_3, f'\left(\xi_3\right)\right)d\xi_3$$

$$\left(Q_1, K_1\right)=\sum_{k=1}^{N}\int_{\frac{-h}{2}}^{\frac{h}{2}}\sigma_5\left(1, f'\left(\xi_3\right)\right)d\xi_3 \qquad (3.13)$$

$$\left(Q_2, K_2\right)=\sum_{k=1}^{N}\int_{\frac{-h}{2}}^{\frac{h}{2}}\sigma_4\left(1, f'\left(\xi_3\right)\right)d\xi_3$$

The differential equations that are given in Eq. (3.12) are further converted into displacements and rotations by undertaking the integrals given as follows:

$$\left[A_{ij} \quad B_{ij} \quad D_{ij} \quad E_{ij} \quad F_{ij} \quad H_{ij}\right]=\int_{-\frac{h}{2}}^{\frac{h}{2}}\left[Q_{ij}^{k}\right]\left[1 \quad \xi_3 \quad {\xi_3}^2 \quad g\left(\xi_3\right) \quad \xi_3.g\left(\xi_3\right) \quad \left(g\left(\xi_3\right)\right)^2\right]d\xi_3 \qquad (3.14)$$

For i, j= 1, 2, 4, 5, and 6.

$$\left[K_{ij} \quad L_{ij}\right]=\int_{-h/2}^{h/2}\left[Q_{ij}^{(k)}\right]_{2x2}\left[g'\left(\xi_3\right) \quad \left(g'\left(\xi_3\right)\right)^2\right]d\xi_3 \quad \text{for } i,j=4,5 \qquad (3.15)$$

After the substitution of Eq. (3.13-15) in Eq. (3.12), the most general form of governing differential equations in the displacement are written as:

$$\left[\overline{R}\right]\{\Delta\} = \{F\} \tag{3.16}$$

where R is an operator matrix for the stiffness coefficients, Δ and F are the generalised displacement and force vectors respectively. For the buckling response the governing equation is expressed as follows:

$$\left|\left[\overline{R}\right] - \lambda[G]\right|\{\Delta\} = \{0\} \tag{3.17}$$

where $[G]$ depicts the geometric matrix due to axial compressive load and λ associates to the buckling parameter which is the solution of Eigen-value problem.

3.6 Solution Methodology

A Naiver-type solution method is utilised for simply supported boundary condition of composite shell panels with the dimension $(a \times b \times h)$and radii of curvatures R_1 and R_2. Moreover, the cross-ply shells are considered for which the following stiffness coefficients are zero.

$A_{i6}=B_{i6}=D_{i6}=E_{i6}=F_{i6}=H_{i6}=0$; ($i$=1,2) (3.18)

$A_{45}=J_{45}=L_{45}=0$

The above characteristics are introduced in the Equation (3.17) and the governing equations for cross-ply shells are obtained as follows:

$$A_{11}\left(\frac{\partial^2 u}{\partial x_1^2}+\frac{1}{R_1}\frac{\partial w}{\partial x_1}\right)+B_{11}\left(\Omega\frac{\partial^2 \phi_1}{\partial x_1^2}-\frac{\partial^3 w}{\partial x_1^3}\right)+E_{11}\left(\frac{\partial^2 \phi_1}{\partial x_1^2}\right)+E_{12}\left(\frac{\partial^2 \phi_2}{\partial x_1 \partial x_2}\right)+A_{12}\left(\frac{\partial^2 v}{\partial x_1 \partial x_2}+\frac{1}{R_2}\frac{\partial w}{\partial x_1}\right)+$$
$$B_{12}\left(\Omega\frac{\partial^2 \phi_2}{\partial x_1 \partial x_2}-\frac{\partial^3 w}{\partial x_1 \partial x_2^2}\right)+A_{66}\left(\frac{\partial^2 v}{\partial x_1 \partial x_2}+\frac{\partial^2 u}{\partial x_2^2}\right)+B_{66}\left(\Omega\left(\frac{\partial^2 \phi_2}{\partial x_1 \partial x_2}+\frac{\partial^2 \phi_1}{\partial x_2^2}\right)-2\frac{\partial^3 w}{\partial x_1 \partial x_2^2}\right)+$$
$$E_{66}\left(\frac{\partial^2 \phi_2}{\partial x_1 \partial x_2}+\frac{\partial^2 \phi_1}{\partial x_2^2}\right)=0$$

$$A_{21}\left(\frac{\partial^2 u}{\partial x_1 \partial x_2}+\frac{1}{R_1}\frac{\partial w}{\partial x_2}\right)+B_{21}\left(\Omega\frac{\partial^2 \phi_1}{\partial x_1 \partial x_2}-\frac{\partial^3 w}{\partial x_1^2 \partial x_2}\right)+E_{21}\left(\frac{\partial^2 \phi_2}{\partial x_2^2}\right)+A_{22}\left(\frac{\partial^2 v}{\partial x_2^2}+\frac{1}{R_2}\frac{\partial w}{\partial x_2}\right)+$$
$$B_{22}\left(\Omega\frac{\partial^2 \phi_2}{\partial x_2^2}-\frac{\partial^3 w}{\partial x_1 \partial x_2^3}\right)+E_{22}\left(\frac{\partial^2 \phi_2}{\partial x_2^2}\right)+A_{66}\left(\frac{\partial^2 v}{\partial x_1^2}+\frac{\partial^2 u}{\partial x_1 \partial x_2}\right)+B_{66}\left(\Omega\left(\frac{\partial^2 \phi_1}{\partial x_1 \partial x_2}+\frac{\partial^2 \phi_2}{\partial x_2^2}\right)-2\frac{\partial^3 w}{\partial x_2 \partial x_1^2}\right)+$$
$$E_{66}\left(\frac{\partial^2 \phi_1}{\partial x_1 \partial x_2}+\frac{\partial^2 \phi_2}{\partial x_1^2}\right)=0$$

$$-\frac{1}{R_1}\left[A_{11}\left(\frac{\partial u}{\partial x_1}+\frac{w}{R_1}\right)+B_{11}\left(\Omega\frac{\partial \phi_1}{\partial x_1}-\frac{\partial^2 w}{\partial x_1^2}\right)+E_{11}\left(\frac{\partial \phi_1}{\partial x_1}\right)+A_{12}\left(\frac{\partial v}{\partial x_2}+\frac{w}{R_2}\right)+B_{12}\left(\Omega\frac{\partial \phi_2}{\partial x_2}-\frac{\partial^2 w}{\partial x_2^2}\right)+E_{12}\left(\frac{\partial \phi_2}{\partial x_2}\right)\right]$$
$$-\frac{N_2}{R_2}+\frac{\partial^2 M_1}{\partial x_1^2}+\frac{\partial^2 M_2}{\partial x_2^2}+2\frac{\partial^2 M_6}{\partial x_1 \partial x_2}=0$$

$$E_{11}\left(\frac{\partial^2 u}{\partial x_1^2}+\frac{1}{R_1}\frac{\partial w}{\partial x_1}\right)+F_{11}\left(\Omega\frac{\partial^2 \phi_1}{\partial x_2^2}-\frac{\partial^3 w}{\partial x_1^3}\right)+H_{11}\left(\frac{\partial^2 \phi_1}{\partial x_1^2}\right)+E_{12}\left(\frac{\partial^2 v}{\partial x_1 \partial x_2}+\frac{1}{R_2}\frac{\partial w}{\partial x_1}\right)$$
$$+F_{12}\left(\Omega\frac{\partial^2 \phi_2}{\partial x_1 \partial x_2}-\frac{\partial^3 w}{\partial x_1 \partial x_2^2}\right)+H_{12}\left(\frac{\partial^2 \phi_2}{\partial x_1 \partial x_2}\right)+\frac{\partial P_6}{\partial x_2}+\Omega\left(\frac{\partial M_1}{\partial x_1}+\frac{\partial M_6}{\partial x_2}\right)-Q_1-K_1=0$$

$$E_{21}\left(\frac{\partial^2 u}{\partial x_1 \partial x_2}+\frac{1}{R_1}\frac{\partial w}{\partial x_2}\right)+F_{21}\left(\Omega\frac{\partial^2 \phi_1}{\partial x_1 \partial x_2}-\frac{\partial^3 w}{\partial x_1^2 \partial x_2}\right)+H_{21}\left(\frac{\partial^2 \phi_2}{\partial x_2^2}\right)+E_{22}\left(\frac{\partial^2 v}{\partial x_2^2}+\frac{1}{R_2}\frac{\partial w}{\partial x_2}\right)$$
$$+F_{22}\left(\Omega\frac{\partial^2 \phi_2}{\partial x_2^2}-\frac{\partial^3 w}{\partial x_2^3}\right)+H_{22}\left(\frac{\partial^2 \phi_2}{\partial x_2^2}\right)+\frac{\partial P_6}{\partial x_1}+\Omega\left(\frac{\partial M_2}{\partial x_2}+\frac{\partial M_6}{\partial x_1}\right)-Q_2-K_2=0$$

(3.19)

The boundary conditions that are used in the present methodology are as follows:

- $v=w=\phi_1=0$ at $x_1=0, a$.
- $u=w=\phi_2=0$ at $x_2=0, b$. (3.20)

These boundary conditions are satisfied by assuming the following series solution:

$$
\begin{aligned}
u &= \sum_{m=1}^{\infty}\sum_{n=1}^{\infty} U_{mn}\cos(\alpha x_1)\sin(\beta x_2);\\
v &= \sum_{m=1}^{\infty}\sum_{n=1}^{\infty} V_{mn}\sin(\alpha x_1)\cos(\beta x_2)\\
w &= \sum_{m=1}^{\infty}\sum_{n=1}^{\infty} W_{mn}\sin(\alpha x_1)\sin(\beta x_2)\\
\phi_1 &= \sum_{m=1}^{\infty}\sum_{n=1}^{\infty} X_{mn}\cos(\alpha x_1)\sin(\beta x_2);\\
\phi_2 &= \sum_{m=1}^{\infty}\sum_{n=1}^{\infty} Y_{mn}\sin(\alpha x_1)\cos(\beta x_2)\\
\alpha &= \frac{m\pi}{a}, \beta = \frac{n\pi}{b}
\end{aligned}
\tag{3.21}
$$

The assumed solution is introduced in the governing equations given by Equation (3.19), simplification leads to U_{mn}, V_{mn}, W_{mn}, X_{mn} and Y_{mn} which are the arbitrary parameters and aid in determining the mid plane displacements and buckling load. The governing system is obtained as $\left|\left[\overline{R}\right]-\lambda\left[G\right]\right|\{\Delta\}=\{0\}$. The matrix R is given in the appendix.

3.7 Modelling and Buckling characteristics of Composite Shells Utilizing Finite Element Method

The multi-layered composite shells are modelled using finite element method. The analytical method has certain limitations such as only simply supported boundary conditions can be imposed and it gives solutions only for cross-ply sequence. Finite element methodology is eligible for both cross-ply and angle-ply composite shells and can be utilized to study the effect of different boundary conditions on these composite shells.

The continuity requirement in the method of finite element suitable for the displacement field of IHSDT represented in Equation (3.1) is C^1 continuity, however, it increases the computational process. In order to obtain the continuity demand to reduced C^0, the derivatives of mid plane transverse deflection are assumed as separate variables. The introduction of two new degrees of freedom (θ_x, θ_y) into the displacement field is given as:

$$\bar{u}(\xi_1,\xi_2,\xi_3) = (1+\frac{\xi_3}{R_1})u + \xi_3\left[\Omega\phi_1 - \frac{\theta_1}{a_1}\right] + f(\xi_3)\phi_1$$

$$\bar{v}(\xi_1,\xi_2,\xi_3) = (1+\frac{\xi_3}{R_2})v + \xi_3\left[\Omega\phi_2 - \frac{\theta_2}{a_2}\right] + f(\xi_3)\phi_2 \qquad (3.22)$$

$$\bar{w}(\xi_1,\xi_2,\xi_3) = w$$

The artificial constraints arise due to the introduction of two separate variables (θ_x, θ_y), are imposed in the system's total potential energy as follows:

$$\frac{\partial w}{\partial \xi_1} - \theta_1 = 0 \qquad \frac{\partial w}{\partial \xi_2} - \theta_2 = 0$$

3.7.1 Strain displacement relations

The strain displacement relation for very small displacement based on this formulation is as follows:

$$\varepsilon_1 = \frac{1}{A_1}\left(\frac{\partial \bar{u}}{\partial \xi_1} + \frac{1}{a_2}\frac{\partial a_1}{\partial \xi_2}\bar{v} + \frac{a_1}{R_1}\bar{w}\right)$$

$$\varepsilon_2 = \frac{1}{A_2}\left(\frac{\partial \bar{v}}{\partial \xi_2} + \frac{1}{a_1}\frac{\partial a_2}{\partial \xi_1}\bar{u} + \frac{a_2}{R_2}\bar{w}\right)$$

$$\varepsilon_4 = \frac{1}{A_2}\frac{\partial \bar{w}}{\partial \xi_2} + A_2\frac{\partial}{\partial \xi_3}\left(\frac{\bar{v}}{A_2}\right) \qquad (3.23)$$

$$\varepsilon_5 = \frac{1}{A_1}\frac{\partial \bar{w}}{\partial \xi_1} + A_1\frac{\partial}{\partial \xi_3}\left(\frac{\bar{u}}{A_1}\right)$$

$$\varepsilon_6 = \frac{A_2}{A_1}\frac{\partial}{\partial \xi_1}\left(\frac{\bar{v}}{A_2}\right) + \frac{A_1}{A_2}\frac{\partial}{\partial \xi_2}\left(\frac{\bar{u}}{A_1}\right)$$

Where,

$$A_1 = \left(1+\frac{\xi_3}{R_1}\right)a_1$$

$$A_2 = \left(1+\frac{\xi_3}{R_2}\right)a_2$$

The parameters ε_1 and ε_2 are normal strains in x_1 and x_2 directions respectively, ε_6 is the in-plane shear strain while ε_4 and ε_5 are the transverse shear strains. $\bar{u}, \bar{v}$ and $\bar{w}$ are the displacements on the surface and a_1 and a_2 represents the vectors tangent to the ξ_1 and ξ_2 coordinate lines.

The generalised strains for the above mentioned normal and shear strains are as follows:

$$\begin{aligned}
\varepsilon_1 &= \varepsilon_1^0 + \xi_3\varepsilon_1^1 + f(\xi_3)\varepsilon_1^2 \\
\varepsilon_2 &= \varepsilon_2^0 + \xi_3\varepsilon_2^1 + f(\xi_3)\varepsilon_2^2 \\
\varepsilon_6 &= \varepsilon_6^0 + \xi_3\varepsilon_6^1 + f(\xi_3)\varepsilon_6^2 \\
\varepsilon_4 &= \Omega\varepsilon_4^0 + f'(\xi_3)\varepsilon_4^3 \\
\varepsilon_5 &= \Omega\varepsilon_5^0 + f'(\xi_3)\varepsilon_5^3
\end{aligned} \tag{3.24}$$

Where,

$$\varepsilon_1^0 = \frac{\partial u}{\partial x_1} + \frac{w}{R_1}, \varepsilon_1^1 = \Omega\frac{\partial \phi_1}{\partial x_1} - \frac{\partial^2 w}{\partial x_2^2}, \varepsilon_1^2 = \frac{\partial \phi_1}{\partial x_1}$$

$$\varepsilon_2^0 = \frac{\partial v}{\partial x_2} + \frac{w}{R_2}, \varepsilon_2^1 = \Omega\frac{\partial \phi_2}{\partial x_2} - \frac{\partial^2 w}{\partial x_2^2}, \varepsilon_2^2 = \frac{\partial \phi_2}{\partial x_2}$$

$$\varepsilon_6^0 = \frac{\partial v}{\partial x_1} + \frac{\partial u}{\partial x_2}, \varepsilon_6^1 = \Omega\frac{\partial \phi_2}{\partial x_1} + \Omega\frac{\partial \phi_1}{\partial x_2} - 2\frac{\partial^2 w}{\partial x_1 \partial x_2}, \varepsilon_6^2 = \frac{\partial \phi_2}{\partial x_1} + \frac{\partial \phi_1}{\partial x_2}$$

$$\varepsilon_4^0 = \phi_2, \varepsilon_4^3 = \phi_2$$

$$\varepsilon_5^0 = \phi_1, \varepsilon_5^3 = \phi_1$$

The strain displacement relation for laminated composite shells are expressed in the form of von-Karman non-linear relations:

$$\{\varepsilon\}_{5\times1} = \{\varepsilon_L\} + \{\varepsilon_{NL}\} \tag{3.25}$$

Where, ε_L and ε_{NL} signifies the linear and non-linear strains separately.

$$\{\varepsilon\}_{5\times1} = \begin{bmatrix}\varepsilon_1 & \varepsilon_2 & \varepsilon_6 & \varepsilon_4 & \varepsilon_5\end{bmatrix}^T$$

$$\{\varepsilon_L\} = \begin{bmatrix}u_{,x} & v_{,y} & u_{,y}\, v_{,x} & v_{,z} + w_{,y} & u_{,z} + w_{,x}\end{bmatrix}^T$$

The non-linear terms that are associated with the buckling behaviour of the composite shells are taken as:

$$\{\varepsilon_{NL}\}=\left[\frac{1}{2}(w,_x)^2 \quad \frac{1}{2}(w,_y)^2 \quad \frac{1}{2}(w,_x)(w,_y) \quad 0 \quad 0\right]^T \tag{3.26}$$

3.7.2 Constitutive Relations

For k_{th} orthotropic layer of composite shell panels, the stress-strain relation of the coordinate system is expressed as:

$$\{\sigma\}_{5\times1}=\left[\overline{Q}_{ij}\right]^{(k)}\{\varepsilon\}_{5\times1} \tag{3.27}$$

where the transformed reduced stiffness matrix is denoted by $\left[\overline{Q}_{ij}\right]$ is constituted of the material properties (E_1 , E_2 , G_{12} , G_{23} , G_{13} and v_{12}).

3.7.3 Element Selection

An element having eight nodes with seven degrees of freedom at each node is taken. The element is an isoperimetric serendipity biquadratic quadrilateral which is used for the meshing of the composite shell. The shape functions at the node i is written as:

$$N_i=\begin{cases}\frac{1}{4}(1+\xi\xi_i)(1+\eta\eta_i)(\xi\xi_i+\eta\eta_i-1) & \text{for } i = 1,2,3,4\\ \frac{1}{2}(1-\xi^2)(1+\eta\eta_i) & \text{for } i= 5,7\\ \frac{1}{2}(1-\eta^2)(1+\xi\xi_i) & \text{for } i = 6, 8\end{cases} \tag{3.28}$$

At each node of the element, the geometry of the element and the field variables for the elements can be stated in the form of shape functions as:

$$\varsigma=\sum_{i=1}^{8}N_i\varsigma_i \qquad \text{and} \qquad q=\sum_{i=1}^{8}N_i q_i \tag{3.29}$$

where ς and q are the generalised geometric coordinate and field variables, respectively, ς_i and q_i are the corresponding coordinate and field variable at the node i.

3.7.4 Derivation of Strain Energies

The generalized linear strain vector $\{\varepsilon\}$ is represented in the following equation:

$$\{\varepsilon_L\}_{5\times1}=[H]_{5\times13}\{\overline{\varepsilon_l}\}_{13\times1} \tag{3.30}$$

Where,

$$\{H\} = \begin{Bmatrix} 1 & 0 & 0 & \xi_3 & 0 & 0 & g(\xi_3) & 0 & 0 & 0 & 0 & 0 & 0 \\ 0 & 1 & 0 & 0 & \xi_3 & 0 & 0 & g(\xi_3) & 0 & 0 & 0 & 0 & 0 \\ 0 & 0 & 1 & 0 & 0 & \xi_3 & 0 & 0 & g(\xi_3) & 0 & 0 & 0 & 0 \\ 0 & 0 & 0 & 0 & 0 & 0 & 0 & 0 & 0 & 1 & 0 & g'(\xi_3) & 0 \\ 0 & 0 & 0 & 0 & 0 & 0 & 0 & 0 & 00 & 0 & 1 & 0 & g'(\xi_3) \end{Bmatrix}$$

and

$$\{\overline{\varepsilon_l}\} = \{\varepsilon_1^0 \quad \varepsilon_2^0 \quad \varepsilon_6^0 \quad \varepsilon_1^1 \quad \varepsilon_2^1 \quad \varepsilon_6^1 \quad \varepsilon_1^2 \quad \varepsilon_2^2 \quad \varepsilon_6^2 \quad \varepsilon_4^0 \quad \varepsilon_4^3 \quad \varepsilon_5^0 \quad \varepsilon_5^3\}$$

Further the generalized strain is represented in terms of field variables as:

$$\{\overline{\varepsilon_l}\}_{13\times1} = \{L\}_{13\times7}\{q\}_{7\times1} \tag{3.31}$$

Where $\{q\}_{7\times1} = [u_0 \quad v_0 \quad w_0 \quad \theta_x \quad \theta_y \quad \phi_x \quad \phi_y]^T$

Using Equation (3.29) in Equation (3.31) the elemental strain-displacement relation can be obtained as follows:

$$\{\overline{\varepsilon_l}\}_j = [B]_j \{q_i\}_j \tag{3.32}$$

The strain energy developed because of the linear strain for the j_{th} element is obtained by using Equation (3.30) and (3.27) and (3.32) as:

$$\begin{aligned} U_l^{(j)} &= \frac{1}{2}\int_v \{\varepsilon_l\}_j^T \{\sigma\} dv = \frac{1}{2}\int_v \{\varepsilon_l\}_j^T [\overline{Q}_{ij}]\{\varepsilon_l\}_j dv = \frac{1}{2}\int_v \{\overline{\varepsilon_l}\}_j^T [H]_j^T [H]_j \{\overline{\varepsilon_l}\}_j dv \\ &= \frac{1}{2}\int_s \{\overline{q}\}_j^T [B]_j^T [D]_j [B]_j \{\overline{q}\}_j dxdy = \frac{1}{2}\{\overline{q}\}_j^T [K_j]\{\overline{q}\}_j \end{aligned} \tag{3.33}$$

To obtain the total strain energy, all the elements are assembled in the form of global displacement vector $\{q\}$ and global stiffness matrix $[K]$:

$$U_l = \sum_{j=1}^{nel} U_l^{(j)} = \frac{1}{2}\{q\}^T [K]\{q\} \tag{3.34}$$

The internal forces i.e. in-plane normal stress and shear are also the constituents of the geometric stiffness matrix. For the formulation of elemental geometric stiffness matrix

nonlinear strain displacement relations are utilized. The strain energy developed due to the nonlinear strains in j_{th} element is as follow:

$$U_{nl}^{(j)} = \frac{1}{2}\int_v \{\varepsilon_{nl}\}_j^T \{\sigma\}_j \, dv = \frac{1}{2}\int_v \{\varepsilon_{nl}\}_j^T [S]\{\varepsilon_{nl}\}_j \, dv$$
$$= \frac{1}{2}\int_v \{\bar{\varepsilon}_{nl}\}_j^T [H_g]_j^T [S][H_g]_j \{\bar{\varepsilon}_{nl}\}_j \, dv \tag{3.35}$$
$$= \frac{1}{2}\int_s \{\bar{q}\}_j^T [B_G]_j^T [G]_j [B_G]_j \{\bar{q}\}_j \, dxdy = \frac{1}{2}\{\bar{q}\}_j^T [K_G]_j \{\bar{q}\}_j$$

Where

$$[G] = \sum_{k=1}^{nl} \int_{Z_l}^{Z_u} [H_G]^T [S][H_G] dz; \qquad S = \begin{bmatrix} S_{xx} & S_{xy} \\ S_{xy} & S_{yy} \end{bmatrix}$$

S_{xx} and S_{yy} are the in-plane stresses and S_{xy} is the in-plane shear. In order to obtain nonlinear strains produced total strain energy, all the elements are assembled to produce global geometric stiffness matrix, $[K_G]$:

$$U_{nl} = \sum_{j=1}^{nel} U_{nl}^{(j)} = \frac{1}{2}\{q\}^T [K_G]\{q\} \tag{3.36}$$

3.7.5 Solution Procedure

For analysing the buckling characteristics of the composite shells, the governing equation is as follows:

$$[K - \lambda K_G]\{q\} = 0 \tag{3.37}$$

Where, K: global stiffness matrix,

K_G: global geometric stiffness matrix,

λ: critical buckling parameter and

q: vector for displacement.

Summary

This chapter aims to formulate the general mathematical model for the proposed problem i.e. the buckling investigation of laminated composite shell structure. The governing equations are

obtained using principle of virtual work. These governing equations are solved in the closed form using a series solution for simply supported boundary conditions and cross-ply lamination sequence. Further, a generalised finite element methodology is developed to analyse the buckling characteristics of laminated composite shells with different boundary conditions and general lamination sequence.

CHAPTER 4

RESULTS AND DISCUSSIONS

4.1 Introduction

In the present section, NDBL of multi-layered curved panels are investigated utilizing the mathematical model presented and the formulation created in the previous chapter. The closed form solution for cross-ply laminates is obtained. The effects of variables like the ratio of radius to span (*R/a*), the thickness proportion (*a/h*), the material anisotropy (E_1/E_2) and the lay-up sequence of the composite shell panels are considered. The composite material properties for the laminated composites that are used are as follows:

Material Properties 1 (MP1):

$E_1 / E_2 = 25$, $G_{12} / E_2 = 0.5$, $G_{13} / E_2 = 0.5$, $G_{23} / E_2 = 0.2$, $\nu_{12} = 0.25$ Reddy (1984)

Material Properties 2 (MP2):

$E_1 / E_2 = 40$, $G_{12} / E_2 = 0.6$, $G_{13} / E_2 = 0.6$, $G_{23} / E_2 = 0.5$, $\nu_{12} = 0.25$ Reddy (1984)

4.2 Buckling Analysis for the Symmetric Cross-Ply Laminated Shells Using Analytical Solution

Before obtaining the results from the computer software code developed, it is necessary to check the correctness of the mathematical model and the developed code in MATLAB. To do so some sample results are obtained from the developed model and are compared with the published results which are discussed in the following section.

4.2.1 Validation of Results

In this section, examination of SSSS cross ply laminated cylindrical shell panels subjected to uniaxial buckling for different thickness proportion is analysed. The supports are simply supported and symmetric cross ply of 5 layer [0˚/90˚/0˚/90˚/0˚] shell is investigated with the properties of material MP2 with *a/b*=1 and radius of curvature as 20. Table 4.1 depicts the value of critical buckling load obtained in the present study and compared with the published results of Nguyen-van *et al*. (2011), Kumar *et al*. (2003) and Prusty and Satsangi (2001). The results are additionally compared with the FSDT given by Sciuva and Carrera (1990).

The NDBL parameter P_{cr} is obtained using the expression below:

$$P_{cr} = \lambda\left(\frac{a^2}{E_2 h^3}\right) \tag{4.1}$$

Table 4.1 Comparison of NDBL with other solutions

Theory	*a/h*				
	10	**20**	**30**	**50**	**100**
Present	24.8153	32.1937	34.1084	35.1802	35.6243
Nguyen-van *et al.* (2011)	24.412	32.557	34.796	36.081	36.656
Kumar *et al.* (2003)	23.97	31.79	-	35.40	36.85
Prusty and Satsangi (2001)	23.96	31.89	33.98	35.39	36.84
FSDT (1990)	24.19	31.91	34.04	35.42	36.86

The results obtained in Table 4.1 using the present theory shows good agreement with the existing results. Moreover, the NDBL increases with the increase in *a/h* ratio.

4.1.2 Spherical Shells Subjected to Uniaxial Load And Biaxial Load (*K1*=1)

A three and four layered spherical shell is subjected to uniaxial and biaxial load having *R/a* ratio as 10 and material properties of MP1. The effect of *a/h* ratio is observed on the NDBL. The results obtained are shown in the Table 4.2. It should be noted that due to increment in *a/h* ratio, the buckling load has a higher value. It can also be seen that the buckling load due to uniaxial load is double of the value due to the biaxial loading. This is due to the fact the higher compressive load enhances the buckling.

Table 4.2 Spherical shell subjected to uniaxial and biaxial load with *R/a*=10 (MP1)

a/h	*Pcr*			
	Uniaxial		**Biaxial**	
	[0°/90°/0°]	**[0°/90°/90°/0°]**	**[0°/90°/0°]**	**[0°/90°/90°/0°]**
5	11.5523	12.8728	5.7762	6.4364
10	22.8416	24.4727	11.4208	12.2363
50	39.7923	39.9752	19.8961	19.9876
100	54.8500	54.9897	27.4250	27.4948

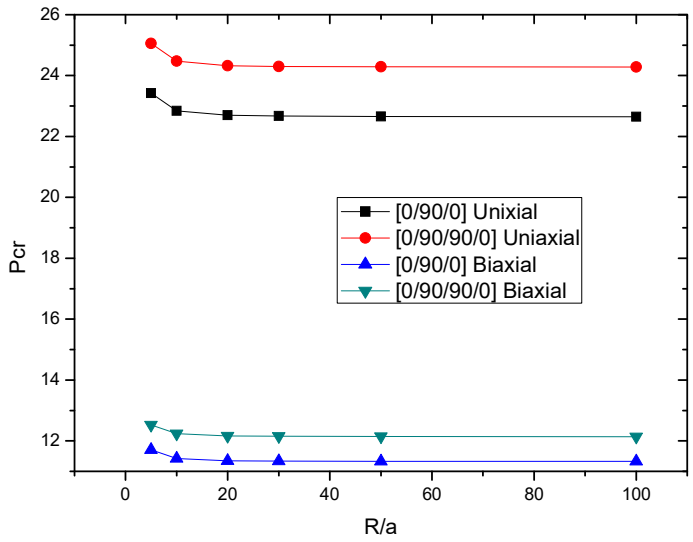

Figure 4.1 NDBL for spherical shell subjected to uniaxial and biaxial load with *a/h*=10

Figure 4.1 represents the NDBL for the spherical shell subjected to uniaxial and biaxial load with *a/h* ratio as 10. The *R/a* ratio is varied to obtain the buckling load value. The material properties are of MP2. It is observed that the NDBL decreases with increase in *R/a* indicating the higher buckling load for the deep shell relative to shallow shell.

4.1.3 Cylindrical Shells Subjected to Uniaxial (K_1=0) and Biaxial Load (K_1=1)

In this section, a three layered and a four layered cylindrical shell subjected to uniaxial and biaxial load is studied. The material properties of each layer is MP1 with the *R/a* ratio of 10. Figure 4.2 depicts the change of buckling load with varying *a/h* ratio. It can be observed that with the increment in *a/h* ratio, the buckling load increases. Figure 4.3 shows the buckling value for shells with *a/h* ratio as 10 and *R/a* is being varied.

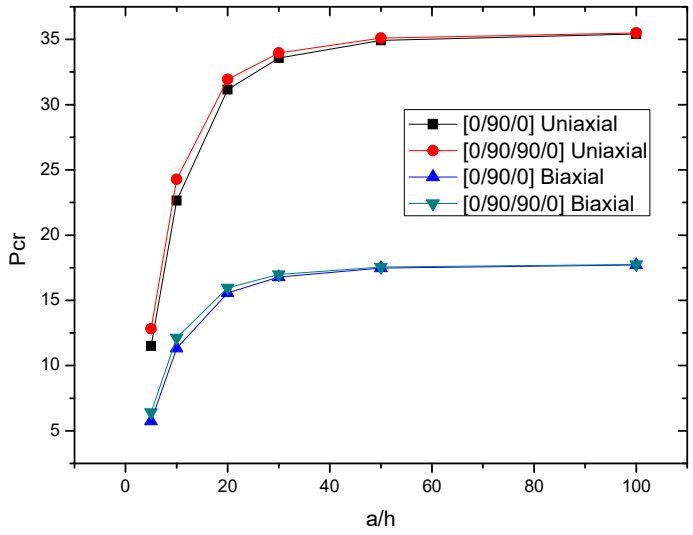

Figure 4.2 NDBL of cylindrical shell subjected to uniaxial and biaxial load with *R/a*=10

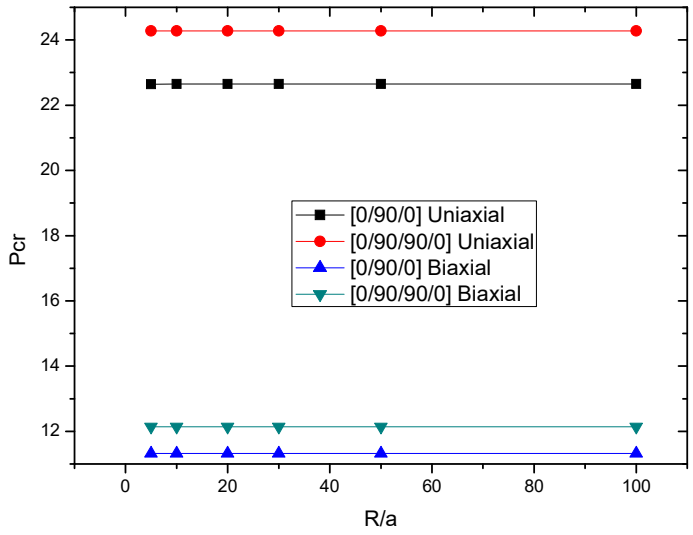

Figure 4.3 NDBL of cylindrical shell subjected to uniaxial and biaxial load with *a/h*=10

4.1.4 Buckling of Shells Subjected to Arbitrary In-Plane Loads

In this segment, the material properties of each layer is of M.P 2. Figure 4.4 represents the varying buckling load with respect to arbitrary in-plane loads of a three and four layered spherical shell. It is clearly observed that the NDBL decreases with the increase in in-plane loads since the compressive forces are increasing in the positive x-direction. The NDBL of cylindrical shell with three and four layers subjected to arbitrary in-plane loads is shown in Figure 4.5.

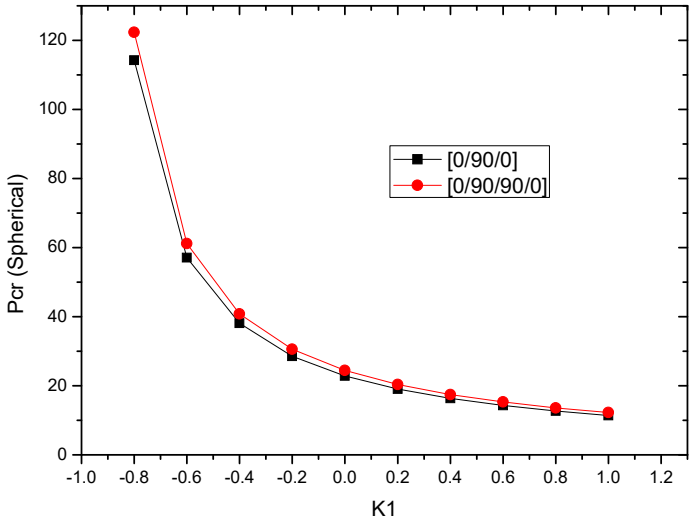

Figure 4.4 Variation of NDBL with arbitrary in-plane load of spherical shell (R_1/a=10, R_2/b=10, a/h=10, MP2)

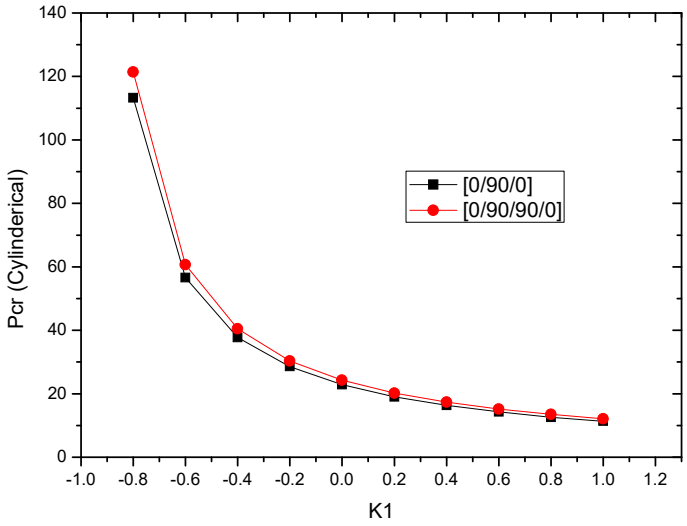

Figure 4.5 Variation of NDBL with arbitrary in-plane load of cylindrical shell (R_1/a=10, R_2/b= ∞, a/h=10, MP2)

4.1.5. Effect of Number of Layers

The NDBL for various increment in layers ([0°/90°/0°], [0°/90°/0°/90°/0°], [0°/90°/0°/90°/0°/90°/0°], [0°/90°/0°/90°/0°/90°/0°/90°/0°] and [0°/90°/0°/90°/0°/90°/0°/90°/0°/90°/0°]) with varying *R/a* and thickness ratio simultaneously is represented in Figure 4.6. Each layer is constituted of material MP2. The results obtained shows the increase in buckling load with number of layers and then becoming constant after certain value. It can also be noted that with the increment in *a/h* ratio, buckling load has also shown the increment significantly.

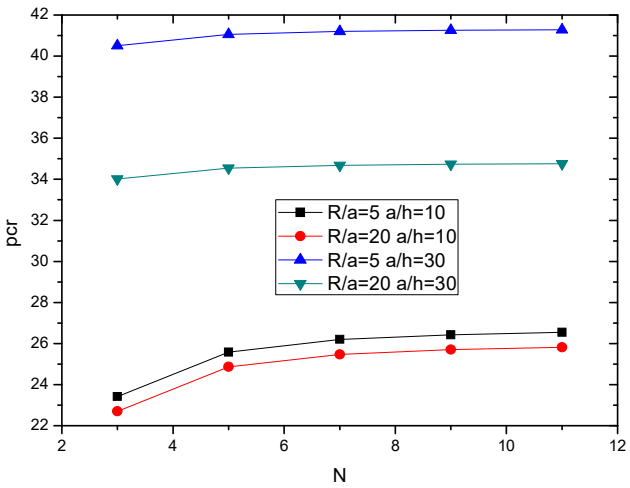

Figure 4.6 Buckling load parameter of spherical shell with different number of layers

4.1.6 Effect of Material Anisotropy (E_1/E_2)

In this section effect of material anisotropy is studied on the buckling load with different number of layers ([0°/90°/0°], [0°/90°/0°/90°/0°], [0°/90°/0°/90°/0°/90°/0°], [0°/90°/0°/90°/0°/90°/0°/90°/0°] and [0°/90°/0°/90°/0°/90°/0°/90°/0°/90°/0°]). A spherical shell having *R/a* as 10 and *a/h* as 10 is considered. Table 4.3 shows that with the increase in E_1/E_2 ratio, the buckling load is increasing.

Table 4.3 Effect of material anisotropy on buckling load for various number of layers

N	E_1/E_2				
	3	**10**	**20**	**30**	**40**
3	5.2531	9.8410	15.1278	19.3585	22.8416
5	5.2631	10.0433	15.8699	20.7881	25.0087
7	5.2669	10.0996	16.0731	21.1843	25.6190
9	5.2681	10.1207	16.1500	21.334	25.8486
11	5.2688	10.1315	16.1891	21.4100	25.9652

4.3 Buckling Analysis of Anti-Symmetric Cross-Ply Laminated Shells

A two-layered shell panel [0°/90°] is considered for analysing the anti-symmetric cross-ply laminated composite shells. Both the layers are of equal thickness and comprises of MP2. Buckling parameter is calculated using the Equation 4.1.

Table 4.4 Effect of radius of curvature on the NDBL of anti-symmetric [0/90]

R/a	**Theory**	P_{cr}
5	Present	12.616
	Librescu et al. (1988) HSDT	12.431
	Librescu et al. (1988) FSDT	12.214
	Librescu et al. (1988) CST	13.877
20	Present	11.766
	Librescu et al. (1988) HSDT	11.610
	Librescu et al. (1988) FSDT	11.406
	Librescu et al. (1988) CST	13.015

Table 4.4 shows the result of non-dimensional buckling parameter for a simply supported spherical panel having span-thickness ratio as 10 and radius of curvature as 5 and 20. The obtained results are compared with the already available results and it can be seen that the present model shows good agreement of results. Table 4.5 indicates the buckling response of anti-symmetric cylindrical shells having *R/a* as 10 for different span to thickness ratios. Shell panels are subjected to both uniaxial and biaxial loading (K_1=1) and each layer is constituted of MP1.

Table 4.5 Effect of span to thickness ratio on the buckling parameter of anti-symmetric [0°/90°] cross ply cylindrical shells.

a/h	P_{cr}	
	uniaxial	***biaxial***
5	6.292	3.146
10	8.332	4.166
20	8.989	4.495
30	9.021	4.510
40	8.944	4.472
50	8.831	4.415
100	8.099	4.049

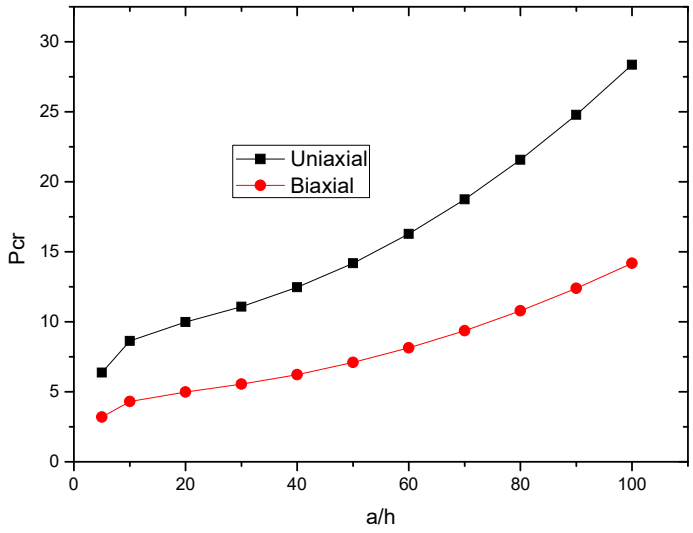

Figure 4.7 Effect of thickness on the buckling load parameter of the anti-symmetric [0°/90°] cross ply spherical shells (MP1, *R/a*=10)

Further, the consequence of span-thickness ratio on the critical NDBL for spherical shells is examined which is illustrated in Figure 4.7. It is observed that with the decrease in thickness of the shell panels the buckling load is increasing. However, the rate of increment is higher for the panel subjected to uniaxial compressive forces.

The consequences of material anisotropy on the buckling parameter is studied for the anti-symmetric cross ply cylindrical and spherical shells and the results are represented in Figure 4.8. Each layer constitutes the property of MP2 with varying E_1/E_2 ratio. It should be noted that the spherical shell is considered as R_1/a=10 and R_2/b=10 while the cylindrical shell is considered as R_1/a=∞ and R_2/b=10. The values which are studied for the distinct modular ratios (E_1/E_2=3,10,20,30 and 40). It can be clearly observed non-dimensional buckling increased as the modular ratio increases. This is accounted towards the increased stiffness of the panel due to increment in E_1/E_2 ratio.

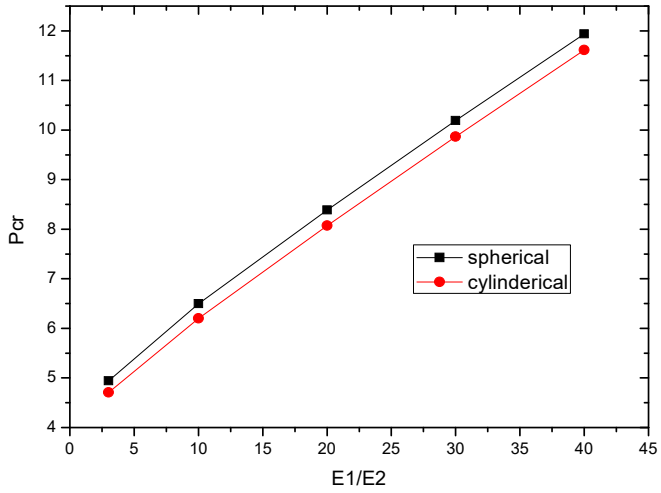

Figure 4.8 Effect of material anisotropy on the critical buckling load for anti-symmetric spherical and cylindrical shells (*a/h*=10, *R/a*=10)

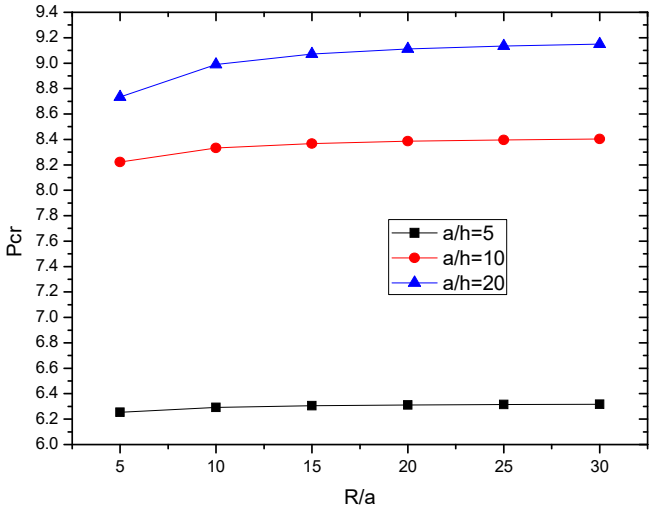

Figure 4.9 Effect of curvature and thickness ratio on the non-dimensional buckling parameter of anti-symmetric [0°/90°] cross ply shells

The non-dimensional buckling parameter is obtained for different curvature ratios having values as *R/a*= 5,10,15,25 and 30 and span-thickness ratio as *a/h*=5,10 and 20 for anti-symmetric cylindrical shells. The layers constitute the properties of MP1. Figure 4.9 illustrates the buckling response of simply supported shell panels. It is already known that with increase in the span-thickness ratio, the shell panel tends to flatten with the increment in the *R/a,* this results in the buckling responses that are constant line.

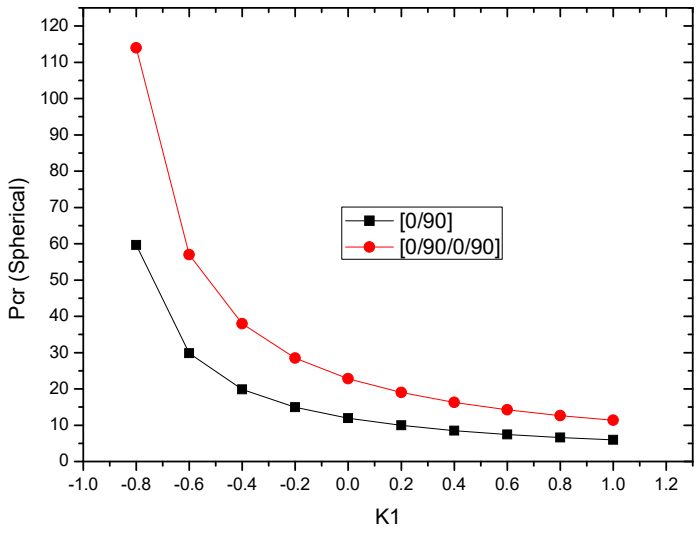

Figure 4.10 Effect of In-plane arbitrary load on NDBL of anti-symmetric spherical shells

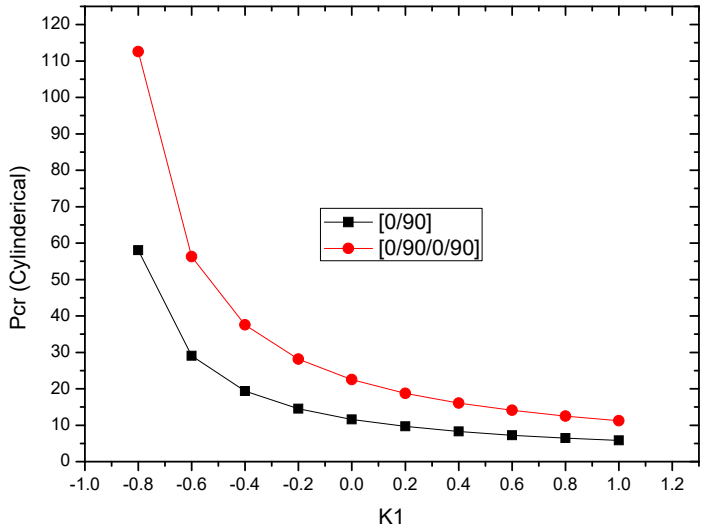

Figure 4.11 Effect of In-plane arbitrary load on NDBL of anti-symmetric cylindrical shells

In the Figure 4.10, the effect of in-plane arbitrary load on non-dimensional buckling load of anti-symmetric spherical shells having radius of curvature as 10 and span-thickness ratio (a/h) as 10 is examined. The study is done for two-layered [0°/90°] and four-layered [0°/90°/0°/90°] spherical shell and each layer is constituted of MP2. Further, the same study is done for the cylindrical shells (R_1/a=10, R_2/b= ∞, a/h=10) in Figure 4.11. It should be clearly noted that the

NDBL decreases with the increment in in-plane loads increasing since the compressive forces are increasing in the positive x-direction.

4.3 Analysis of Multi Layered Composite Shell Panels Employing FEM

In this section, the formulated finite element model using inverse hyperbolic shear deformation theory is analysed and compared with the previously obtained results of closed form solutions for simply supported boundary conditions. In order to obtain the results, a generalised MATLAB code is prepared for the present finite element model. There are two boundary conditions that are used for the present model:

1. Clamped boundary condition (CC): $u_0 = v_0 = w_0 = \phi_x = \phi_y = \theta_x = \theta_y = 0$
2. Simply supported boundary condition (SS):

   $u_0 = w_0 = \phi_x = \theta_x = 0$ at x=0, a

   $v_0 = w_0 = \phi_y = \theta_y = 0$ at y=0, b

4.3.1 Convergence Study of Buckling Parameter

The convergence of the present model is checked by evaluating the NDBL parameter of a four layered [0°/90°/90°/0°] composite spherical shell. The thickness ratio is taken as 10 and *R/a* is taken as 10. The material properties of each layer is constituted of MP1.

In Figure 4.12. It is illustrated that the solution is well converged. The results of buckling parameter are obtained for different boundary conditions (SSSS, CCCC and SCSC) for mesh size range from 2 to 12. It is concluded that mesh size 10 is sufficient for the prediction of buckling behaviour.

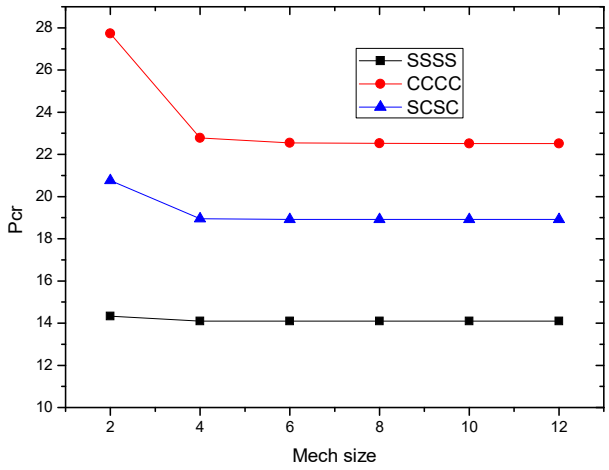

Figure 4.12 Convergence of NDBL for uni-axial symmetric cross ply spherical shells

The convergence study is further done for the 5-layered [0°/90°/0°/90°/0°] symmetric cross-ply cylindrical shells. The span to thickness ratio is 10 and radius of curvature is also 10. Each layer of the laminate constitutes of MP2. In Figure 4.13, the non-dimensional bi-axial buckling load is obtained for different boundary conditions.

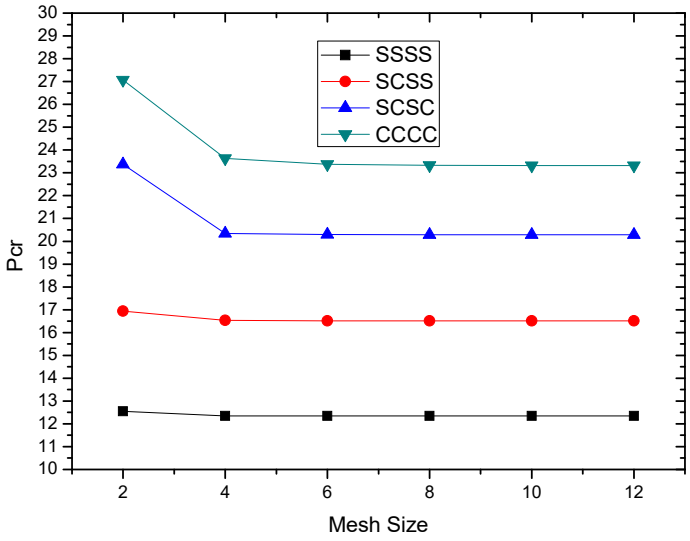

Figure 4.13 Convergence of NDBL for bi-axial symmetric cylindrical cross ply shells

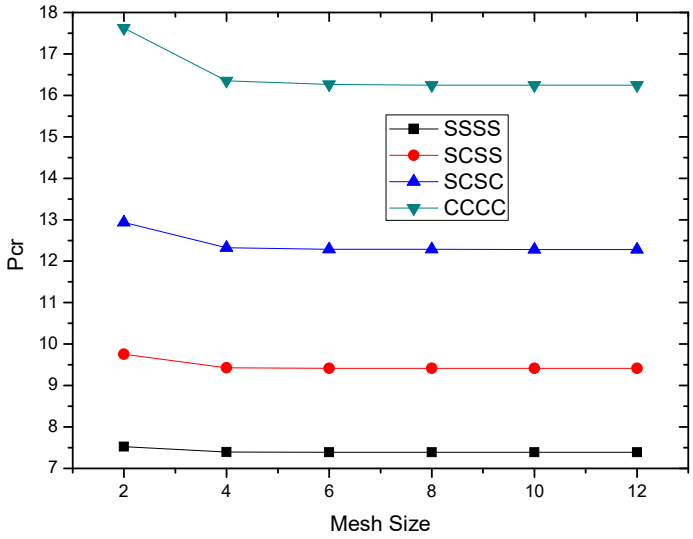

Figure 4.14 Convergence of NDBL for bi-axial anti-symmetric spherical cross ply

The convergence study of anti-symmetric spherical shell [0°/90°] of span to thickness as 10 and radius of curvature is 20 is also performed. The material property of each laminate is MP1.

In Figure 4.14, the results are well converged for different boundary conditions. For further analysis, a mesh size of 10 is considered.

4.3.2 Buckling of Symmetric Cross-Ply Shells

4.3.2.1 Validation of Results

A simply supported 5-layered [0°/90°/0°/90°/0°] cylindrical shell having radius of curvature as 20 is considered. The effect span to thickness ratio on the uniaxial non-dimensional buckling load is studied in the Table 4.6 and the results are contrasted with the value of critical buckling load of the existing results of Nguyen-van *et al*. (2011), Kumar *et al*. (2003) and Prusty and Satsangi (2001). The results are also contrasted with the FSDT given by Sciuva and Carrera (1990). It is concluded that the FEM results from the present work shows satisfying agreement with the available results.

Table 4.6 Non-dimensional buckling load of [0°/90°/0°/90°/0°] cylindrical shell (MP2)

Theory	*a/h*				
	10	**20**	**30**	**50**	**100**
Present (FEM)	24.6440	32.3763	34.4692	35.8409	37.4232
Nguyen-van *et al.* (2011)	24.412	32.557	34.796	36.081	36.656
Kumar *et al.* (2003)	23.97	31.79	-	35.40	36.85
Prusty and Satsangi (2001)	23.96	31.89	33.98	35.39	36.84
FSDT (1990)	24.19	31.91	34.04	35.42	36.86

4.3.2.2 Analysis of Spherical Shells

The NDBL parameter is evaluated for the 3-layered [0°/90°/0°] and 4-layered [0°/90°/90°/0] spherical shells. The layers are constituted of MP2. The variation of span to thickness is studied for the shells having curvature ratio equal to 10.

Table 4.7 Comparison of NDBL for symmetric three and four layered spherical shells of finite element and closed form solution

a/h	P_{cr} (CFS)		P_{cr} (FEM)	
	[0°/90°/0°]	[0°/90°/90°/0°]	[0°/90°/0°]	[0°/90°/90°/0°]
5	11.2165	12.2621	10.9935	11.9803
10	22.4989	23.8094	22.3749	23.5972
50	40.9531	41.1191	40.9458	41.1032
100	58.7753	58.9488	58.7787	58.9500

In Table 4.7, the results obtained for non-dimensional buckling parameter are compared with the results obtained from the analytical solution. It should be noted that it shows good agreement with the closed form solution. Further in Figure 4.15, the effect of different boundary conditions over the NDBL parameter is studied for various span-thickness ratio as *a/h*=5,10,20,50 and 100 and radius of curvature as *R/a*= 20.

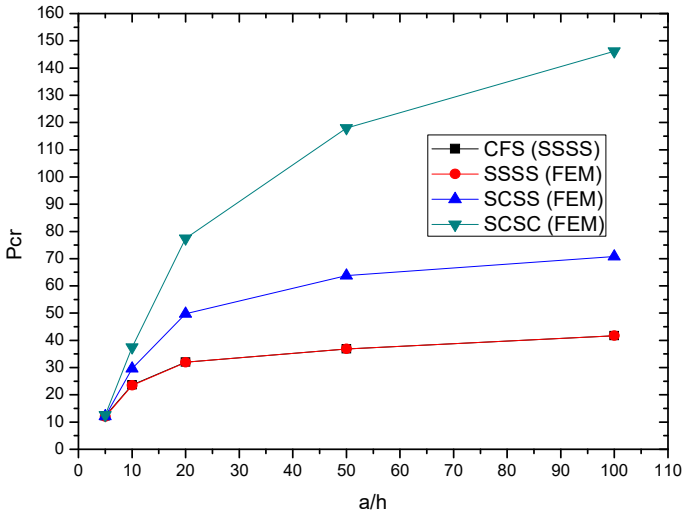

Figure 4.15 NDBL of 4-layered spherical shell for different boundary conditions and comparison with closed form solution

It can be clearly observed from Figure 4.15 that the results for simply supported spherical shells using analytical method shows good agreement with that one of the finite element. Further, with different boundary conditions it can be seen that the shell with two edges being clamped shows higher buckling load rather than the one with one clamped edge. The higher buckling

load for the clamped condition is accounted towards the increased stiffness due to clamped boundary.

4.3.2.3 Analysis of Cylindrical Shells

The NDBL parameter is obtained for the 3-layered [0°/90°/0°] and 4-layered [0°/90°/90°/0] cylindrical shells. The layers are constituted of MP2. The variation of span to thickness is studied over the shells having curvature equal to 10. In Table 4.8, the results obtained for non-dimensional buckling parameter are compared with the results obtained from the analytical solution. It can be observed that the results show good match with the closed form solution.

Table 4.8 Comparison of non-dimensional buckling load for symmetric three and four layered cylindrical shells of finite element and closed form solution.

a/h	P_{cr} (CFS)		P_{cr} (FEM)		% error	
	[0/90/0]	[0/90/90/0]	[0/90/0]	[0/90/90/0]	[0/90/0]	[0/90/90/0]
5	11.1612	12.2066	10.9507	11.9372	2.389	2.298
10	22.2776	23.5874	22.2035	23.4248	4.881	0.891
50	35.4205	35.5671	36.6611	36.7921	0.0178	0.0385
100	36.6446	36.7409	41.6398	41.7055	0.0057	0.0057

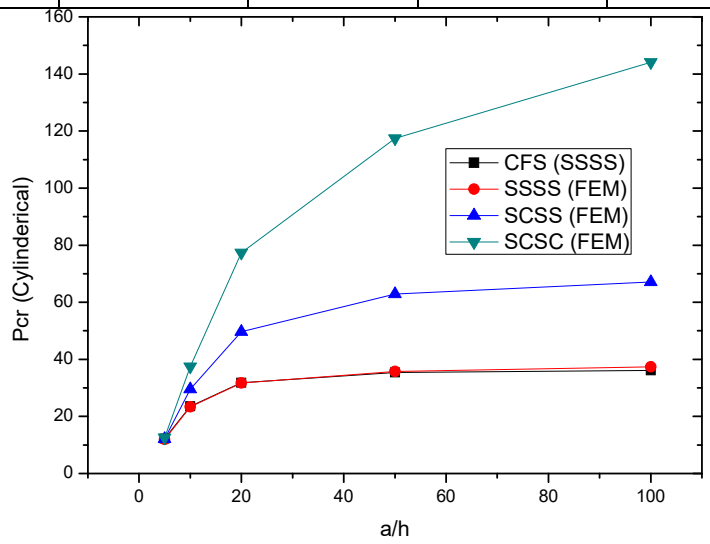

Figure 4.16 Non-dimensional buckling load of 4-layered cylindrical shell for different boundary conditions and comparison with closed form solution

Further in Figure 4.16, the effect of different boundary conditions over the NDBL parameter for cylindrical shell is examined for various span-thickness ratio as *a/h*=5,10,20,50 and 100 and radius of curvature as *R/a*= 20. It can be clearly observed from Figure 4.16 that the results for SSSS spherical shells using analytical method shows good agreement with that one of the finite element. Further, with different boundary conditions it can be observed that the shell with two edges being clamped shows higher buckling load rather than the one with one clamped edge.

4.3.3 Buckling of Anti-Symmetric Cross-Ply Shells

A two-layered shell panel [0°/90°] is considered for analysing the anti-symmetric cross-ply composite shells. Both the layer is of equal thickness and comprises of MP2. Buckling response is calculated using the Equation 4.1.

Table 4.9 Effect of radius of curvature on the NDBL of anti-symmetric [0°/90°] simply supported spherical shells and compared with the finite element method and closed form solution

R/a	Theory	P_{cr}
5	Present (FEM)	12.4583
	Present (CFS)	12.616
	Librescu et al. (1988) HSDT	12.431
	Librescu et al. (1988) FSDT	12.214
	Librescu et al. (1988) CST	13.877
20	Present (FEM)	11.6076
	Present (CFS)	11.766
	Librescu et al. (1988) HSDT	11.610
	Librescu et al. (1988) FSDT	11.406
	Librescu et al. (1988) CST	13.015

Table 4.9, shows the result of NDBL parameter for a simply supported spherical panel having span-thickness ratio as 10 and radius of curvature as 5 and 20. The obtained results are compared with the already available results and it can be seen that the present model shows good agreement of results

Further, anti-symmetric cross-ply spherical shell having radius of curvature 50 is considered. The lay-up sequence is as [0°/90°], [0°/90°/0°/90°], [0°/90°/0°/90°/0°/90°] and [0°/90°/0°/90°/0°/90°/0°/90°]. Each layer constitutes the properties of MP2.

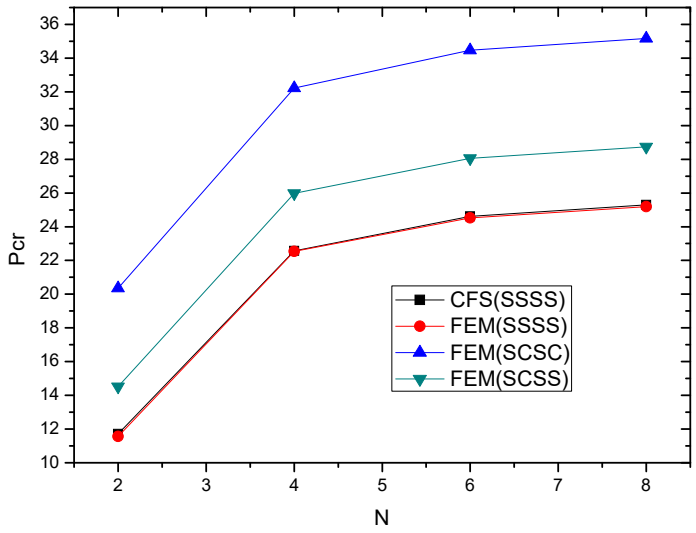

Figure 4.17 NDBL of anti-symmetric spherical shells and comparison with closed form solution

The effect of increase in number of layers on the non-dimensional uniaxial buckling load is illustrated in Figure 4.17. The analytical solution for the simply supported shell shows good agreement with the finite element result of simply supported condition. As for the different boundary conditions it can be observed that the shell with two edges being clamped shows higher buckling load rather than the one with one clamped edge.

Summary

The buckling response of cross-ply composite shells is studied by adopting both the methods viz. analytical and finite element formulation. The inverse hyperbolic shear deformation theory was implemented for the modelling of shell structure. The effect of radius of curvature, lay-up scheme, material anisotropy and span-thickness ratio is studied for the both spherical and

cylindrical shells. The comparison of analytical solution with the finite element method is also illustrated.

CHAPTER 5

CONCLUSIONS AND SCOPE FOR FUTURE WORK

5.1 Conclusions

The critical buckling of composite cylindrical and spherical shells under the frame work of IHSDT is being studied subjected both uni-axial and bi-axial loading. A general MATLAB code was formulated on the basis of mathematical model developed. Further, finite element method was implemented for the study of critical buckling load and the values are obtained solving the Eigen value problem. The parametric study is done for the various combinations such lay-up scheme, material anisotropy, radius of curvature and span to thickness ratio subjected to various boundary conditions. On the basis of the present work, the following conclusions can be drawn:

1. The buckling response for cross-ply spherical and cylindrical shells subjected to uni-axial and bi-axial load is obtained using analytical and finite element method.
2. The increment in the span-thickness ratio results in the increase in buckling load parameter in both spherical and cylindrical shells as increasing the span-thickness ratio the shell becomes thin and experiences more buckling load.
3. The increase in radius of curvature, the value of buckling load does not seem to change significantly.
4. The in-plane load increment results in the decrease of buckling load in both cylindrical and spherical shells since the compressive forces are increasing in the positive x-direction.
5. The increase in buckling load with number of layers and then becoming constant after a certain value can be observed.
6. The material anisotropy increment results in the increase of buckling load of symmetric and anti-symmetric laminated shells.

Following research papers are prepared on the basis of present work:

1. Neeraj H, Rajpoot R, Grover N, Khanna K. Buckling of laminated composite plates using IHSDT subjected to in-plane arbitrary loads. 3rd Indian Conference on Applied Mechanics -2018 BITS Pilani, K. K. Birla Goa Campus. 31-32

2. Neeraj H, Grover N, Khanna K. Analytical modelling of shell structure for buckling load characteristics using inverse hyperbolic shear deformation theory. (Under preparation)
3. Neeraj H, Grover N, Khanna K. Finite element evaluation and modelling of composite shells for buckling using inverse hyperbolic shear deformation theory. (Under preparation)

5.2 Scope for Future Work

1. The influence of thermal environment on the buckling characteristics of laminated composite shells.
2. The non-linear finite element analysis of buckling characteristics of shell structure of composite material.
3. The critical buckling response of advanced composite shell structure.
4. Effect of the buckling response characteristics on the arbitrary geometry of composite shell structure.

REFERENCES

Carrera, E. (2002). Theories and finite elements for multilayered, anisotropic, composite plates and shells. *Archives of Computational Methods in Engineering*, *9*(2), 87-140.

Fazzolari, F. A., Banerjee, J. R., and Boscolo, M. (2013). Buckling of composite plate assemblies using higher order shear deformation theory-an exact method of solution. *Thin-Walled Structures*, 71, 18-34.

Ferreira, A. J. M., and Barbosa, J. T. (2000) Buckling behaviour of composite shells. *Composite Structures,* 50(1), 93-98.

Ferreira, A. J. M., Roque, C. M. C., Neves, A. M. A., Jorge, R. M. N., Soares, C. M. M., and Liew, K. M. (2011). Buckling and vibration analysis of isotropic and laminated plates by radial basis functions. *Composites Part B: Engineering*, *42*(3), 592-606.

Grover, N., Maiti, D. K., and Singh, B. N. (2013). A new inverse hyperbolic shear deformation theory for static and buckling analysis of laminated composite and sandwich plates. *Composite Structures*, 95, 667-675.

Grover, N., Singh, B. N., and Maiti, D. K. (2013). Analytical and finite element modelling of laminated composite and sandwich plates: An assessment of a new shear deformation theory for free vibration response. *International Journal of Mechanical Sciences*, 67, 89-99.

Grover, N., Singh, B. N., and Maiti, D. K. (2014). A general assessment of a new inverse trigonometric shear deformation theory for laminated composite and sandwich plates using finite element method. *Proceedings of the Institution of Mechanical Engineers*, *Part G: Journal of Aerospace Engineering*, 228(10), 1788-1801.

Joshan, Y. S., Grover, N., and Singh, B. N. (2017). Analytical modelling for thermo-mechanical analysis of cross-ply and angle-ply laminated composite plates. *Aerospace Science and Technology,* 70, 137-151.

Joshan, Y. S., Grover, N., and Singh, B. N. (2017). A new non-polynomial four variable shear deformation theory in axiomatic formulation for hygro-thermo-mechanical analysis of laminated composite plates. *Composite Structures*, 182, 685-693.

Khanna, K., Gupta, V. K., and Nigam, S. P. (2015). Creep analysis of a variable thickness rotating FGM disc using Tresca criterion. *Defence Science Journal*, 65(2), 163-170.

Khanna, K., Gupta, V. K., and Nigam, S. P. (2017). Modelling and analysis of creep in a variable thickness rotating FGM disc using Tresca and Von Mises criteria. *Iranian Journal of Science and Technology, Transactions of Mechanical Engineering*, 41(2), 109-119.

Khdeir, A. A., Reddy, J. N., and Frederick, D. (1989). A study of bending, vibration and buckling of cross-ply circular cylindrical shells with various shell theories. *International Journal of Engineering Science,* 27(11), 1337-1351.

Koiter, W. (1960). A consistent first approximation in the general theory of thin elastic shells. *Theory of Thin Elastic Shells*, 12-33.

Kumar, L. R., Datta, P. K., and Prabhakara, D. L. (2003). Tension buckling and dynamic stability behaviour of laminated composite doubly curved panels subjected to partial edge loading. *Composite Structures,* 60(2), 171-181.

Love, A. E. H. (1927) The mathematical theory of elasticity.

Mantari, J. L., Oktem, A. S., and Soares. C. G. (2011). Static and dynamic analysis of laminated composite and sandwich plates and shells by using a new higher-order shear deformation theory. *Composite structures,* 94(1) 37-49.

Mantari, J. L., Oktem, A. S., and Soares, C. G. (2012). A new trigonometric shear deformation theory for isotropic, laminated composite and sandwich plates. *International Journal of Solids and Structures*, 49(1), 43-53.

Mantari, J. L., Oktem, A. S., and Soares, C. G. (2012). A new higher order shear deformation theory for sandwich and composite laminated plates. *Composites Part B: Engineering*, 43(3), 1489-1499.

Nguyen-Van, H., Mai-Duy, N., Karunasena, W., and Tran-Cong, T. (2011). Buckling and vibration analysis of laminated composite plate/shell structures via a smoothed quadrilateral flat shell element with in-plane rotations. *Computers and Structures*, 89(7-8), 612-625.

Pagano, N. J., (1970). Exact solutions for rectangular bidirectional composites and sandwich plates. *Journal of Composite Materials,* 4(1), 20-34.

Prusty, B. G., and Satsangi, S. K. (2001). Finite element transient dynamic analysis of laminated stiffened shells. *Journal of Sound and Vibration,* 248(2), 215-233.

Reddy, J. N., and Liu, C. F. (1985). A higher-order shear deformation theory of laminated elastic shells. *International Journal of Engineering Science,* 23(3), 319-330.

Reissner, E. (1945). The effect of transverse shear deformation on the bending of elastic plates. *Journal of applied Mechanics*, A69-A77.

Reissner, E., and Stavsky, Y. (1961). Bending and stretching of certain types of heterogeneous aeolotropic elastic plates. *Journal of Applied Mechanics*, 28(3), 402-408.

Srinivas, S., and Rao, A. K. (1970). Bending, vibration and buckling of simply supported thick orthotropic rectangular plates and laminates. *International Journal of Solids and Structures,* 6(11), 1463-1481.

Shadmehri, F., Hoa, S. V., and Hojjati, M. (2012). Buckling of conical composite shells. *Composite Structures*, 94(2), 787-792.

Sundaresan, P., Singh, G., and Rao, V. (1998). Buckling of moderately thick rectangular composite plates subjected to partial edge compression. *International Journal of Mechanical Sciences,* 40(11), 1105-1117.

Thinh, T. I. (2005). Buckling analysis of laminated cylindrical composite shell panel under mechanical and hygrothermal loads. *Vietnam Journal of Mechanics*, 27(1), 1-12.

Appendix

The elements of [R] matrix:

$$R_{11} = \left[A_{11}\alpha^2 + A_{66}\beta^2\right], R_{12} = \left[(A_{12} + A_{66})\alpha\beta\right]$$

$$R_{13} = -(A_{11}\frac{\alpha}{R_1} + A_{12}\frac{\alpha}{R_2} + B_{11}\alpha^3 + B_{12}\alpha\beta^2 + 2B_{66}\alpha\beta)$$

$$R_{14} = \left[(\Omega B_{11} + E_{11})\alpha^2 + E_{66}\beta^2 + \Omega B_{66}\beta^2\right]$$

$$R_{15} = \left[\Omega B_{12} + E_{12} + \Omega B_{66} + E_{66}\right]\alpha\beta$$

$$R_{22} = \left[A_{22}\beta^2 + A_{66}\alpha^2\right]$$

$$R_{23} = -\left(A_{21}\frac{\beta}{R_1} + A_{22}\frac{\beta}{R_2} + B_{11}\alpha^3 + B_{21}\alpha^2\beta + B_{22}\beta^3 + 2B_{66}\alpha\beta\right)$$

$$R_{24} = \left[\Omega B_{21} + E_{21} + \Omega B_{66} + E_{66}\right]\alpha\beta$$

$$R_{25} = \left[(\Omega B_{22} + E_{22})\beta^2 + (\Omega B_{66} + E_{66})\alpha^2\right]$$

$$R_{33} = -\left(\begin{array}{l}\frac{A_{11}}{R_1^2} + \frac{2}{R_1R_2}A_{12} + \frac{2\alpha^2}{R_1}B_{11} + \frac{\beta^2}{R_1}B_{12} + \frac{\alpha^2}{R_2}B_{21} + \frac{\beta^2}{R_2}B_{22} + \frac{\beta^2}{R_2}B_{12} \\ + \frac{\beta^2}{R_1}B_{21} + \frac{\beta^2}{R_2}B_{22} + (D_{11} + D_{12} + D_{21} + 2D_{66})\alpha^2\beta^2 + D_{22}\beta^4\end{array}\right)$$

$$R_{34} = \left[\begin{array}{l}\Omega\alpha\left(\frac{B_{11}}{R_1} + \frac{B_{21}}{R_2}\right) + \alpha\left(\frac{E_{11}}{R_1} + \frac{E_{21}}{R_2}\right) + \alpha^3(F_{11} + \Omega D_{11}) \\ + \alpha\beta^3(\Omega D_{21} + F_{21} + 2\Omega D_{66} + 2F_{66})\end{array}\right]$$

$$R_{35} = \left[\begin{array}{l}\left(\frac{B_{12}}{R_1} + \frac{B_{22}}{R_2}\right)\Omega\beta + \left(\frac{E_{12}}{R_1} + \frac{E_{22}}{R_2}\right)\beta \\ + (\Omega D_{12} + F_{12} + 2\Omega D_{66} + 2F_{66})\alpha^2\beta + (\Omega D_{22} + F_{22})\beta^3\end{array}\right]$$

$$R_{44} = \left[\alpha^2(\Omega F_{11} + H_{11} + \Omega^2 D_{11} + \Omega F_{11}) + \beta^2(H_{66} + \Omega^2 D_{66} + 2\Omega F_{66}) - A_{55} - 2J_{55} - L_{55}\right]$$

$$R_{45} = \left[\Omega F_{12} + H_{12} + \Omega F_{66} + H_{66} + \Omega^2 D_{12} + \Omega F_{12} + \Omega^2 D_{66}\right]\alpha\beta$$

$$R_{55} = \left[\beta^2(\Omega F_{22} + H_{22} + \Omega D_{22} + \Omega F_{22}) + \alpha^2(2\Omega F_{66} + H_{66} + \Omega^2 D_{66}) - A_{44} - 2J_{44} - L_{44}\right]$$

Turnitin Originality Report

Processed on: 16-Jul-2018 23:17 +0530
ID: 833254136
Word Count: 7439
Submitted: 4

Honey Thesis By Kishore Khanna

Similarity Index	Similarity by Source	
18%	Internet Sources:	6%
	Publications:	17%
	Student Papers:	3%

1% match (Internet from 22-Dec-2012)
http://www.arpapress.com/Volumes/Vol8Issue2/IJRRAS_8_2_09.pdf

1% match (Internet from 09-Dec-2014)
http://eprints.usq.edu.au/20438/4/Nguyen-Van_Mai-Duy_Karunasena_Tran-Cong_CS_2011a_AV.pdf

1% match (publications)
Y.S. Joshan, Neeraj Grover, B.N. Singh, "Analytical modelling for thermo-mechanical analysis of cross-ply and angle-ply laminated composite plates", Aerospace Science and Technology, 2017

1% match (publications)
Neeraj Grover, Bhrigu N Singh, Dipak K Maiti, "Free vibration and buckling characteristics of laminated composite and sandwich plates implementing a secant function based shear deformation theory", Proceedings of the Institution of Mechanical Engineers, Part C: Journal of Mechanical Engineering Science, 2014

1% match (publications)
Pankaj V Katariya, Subrata Kumar Panda, "Thermal buckling and vibration analysis of laminated composite curved shell panel", Aircraft Engineering and Aerospace Technology, 2016

1% match (publications)
Grover, Neeraj, D.K. Maiti, and B.N. Singh, "A new inverse hyperbolic shear deformation theory for static and buckling analysis of laminated composite and sandwich plates", Composite Structures, 2013.

1% match (publications)
Structural Vibration, 2015.

< 1% match (publications)
Grover, Neeraj, B.N. Singh, and D.K. Maiti, "Analytical and finite element modeling of laminated composite and sandwich plates: An assessment of a new shear deformation theory for free vibration response", International Journal of Mechanical Sciences, 2013.

< 1% match (Internet from 14-Jun-2016)
http://www.scielo.br/scielo.php?script=sci_arttext&pid=S1679-78252014000700011&lang=es

< 1% match (publications)